MODULATING INSULIN SIGNALING AND TRAFFICKING IN BLOOD-BRAIN BARRIER ENDOTHELIAL CELLS USING LIPID NANOEMULSIONS

A DISSERTATION

SUBMITTED TO THE FACULTY OF THE UNIVERSITY OF MINNESOTA

BY

LUSHAN WANG

IN PARTIAL FULFILLMENT OF THE REQUIREMENTS

FOR THE DEGREE OF

MASTER OF SCIENCE

KARUNYA K. KANDIMALLA

FEBRUARY 2022

ACKNOWLEDGEMENTS

A few years ago, I boarded a plane heading to Minneapolis, MN, USA, and started my academic career in pharmaceutics with little knowledge of what was ahead of me as an undergraduate intern. I have been fortunate enough to meet many people who have supported me along my journey to this point in various aspects, and I am forever in debt for their help.

My advisor, Professor Karunya Kandimalla, deserves special thanks for his continuous support and guidance in my study of Alzheimer's disease. It was Dr. Kandimalla who encouraged me and pulled me out of my misery when I was struggling with my personal life in 2019. He was so generous with his time that it seemed he was always available. His enthusiasm for science is inspiring, and it has gradually ignited my genuine interest and curiosity in my research.

I also want to thank my co-advisor, Dr. Timothy Wiedmann, for sharing his knowledge in the physical pharmaceutical field. Throughout my studies, he patiently evaluated and revised my manuscripts/papers, answered my questions, and provided constructive insights on my work.

Many thanks to Professor Weihua Guan, one of my committee members. Although I only took one course from him, his biostatistics lectures enabled me to accomplish so much in this thesis.

I would like to express my gratitude to my pharmaceutics department colleagues, especially Drs. Ronald Siegel, William Elmquist, Raj Suryanarayanan, and Changquan Calvin Sun, for their support during my first year as a master student. My gratitude also extends to my friends who accompanied me, comforted me, and brought me love and joy since the pandemics. I wish them the best of luck in their future endeavors.

Last but not least, I want to express my gratitude to my family, especially my parents and grandma, for their unshakable love, as well as my fiancé, Liang Zhu, for sharing my life, shouldering my burden, and cheering me up.

ABSTRACT

The compositionally distinct lipid rafts present in the plasma membrane regulates the restrictive trafficking and signal transduction in the blood-brain barrier (BBB) endothelium. Several devastating metabolic and neurodegenerative diseases are associated with lipid homeostasis disruption within the BBB endothelium. Here, we hypothesized that the delivery of lipid nanoemulsions containing unsaturated fatty acids (UFAs) provides a novel approach for disease modification by modulating lipid raft integrity and correcting the aberrant trafficking and signal transduction. Western blot and flow cytometry analysis showed that soybean oil nanoemulsions (SNEs) containing polyunsaturated fatty acids (PUFAs) increased insulin uptake and phospo-AKT (p-AKT) expression, which is a marker for the stimulation of metabolic arm of the insulin signaling, in human cerebral microvascular endothelial cell line (hCMEC/D3) monolayers. Moreover, the use of Alex Fluor 647 labelled cholera toxin (AF647-CXT) in polarized hCMEC/D3 cell monolayers demonstrated that SNEs alter lipid raft morphology, which highlights the role of PUFAs-enriched SNEs in the regulation of lipid rafts. However, olive oil nanoemulsions (ONEs) containing monounsaturated fatty acids (MUFAs) had no detectable impact on lipid raft integrity, AKT phosphorylation, or insulin uptake. These findings provided direct evidence that nanoemulsions containing PUFAs can upregulate the insulin-pAKT pathway and facilitate insulin trafficking at the BBB. Therefore, SNEs may provide a novel nano-strategy to modulate cerebrovascular function in metabolic and neurodegenerative diseases.

KEYWORDS: unsaturated fatty acid, soybean oil, olive oil, nanoemulsions, lipid rafts, insulin resistance, insulin signaling, insulin trafficking

TABLE OF CONTENTS

LIST OF TABLES

LIST OF FIGURES

1. Introduction

The blood-brain barrier (BBB) is the continuous, non-fenestrated microvasculature of the central nervous system (CNS), which precisely regulates the movement of solutes between the blood and the brain parenchyma. The BBB endothelial cells are the major contributor to tightly regulate CNS homeostasis, which is important for maintaining proper neuronal functions and protecting CNS from toxins, inflammation, pathogens, and diseases (Daneman and Prat 2015). Increasing evidence shows that the CNS contributes to the regulation of systemic metabolism and lipid balance. The CNS has a unique lipidomic profile and maintaining its unique lipid composition is critical for restrictive trafficking and signal transduction in the BBB endothelium (Andreone, Chow et al. 2017).

Several metabolic and neurodegenerative diseases are associated with lipid imbalance within the BBB endothelium. Lipid imbalance in the CNS includes alteration in lipid uptake, lipid raft, and lipid-related alteration of BBB cell membrane fluidity. In addition, recent studies have hilighted the potential ability of dietary supplement of "good" lipids into the peripheral and brain to treat metabolic or neurodegenerative disorders. However, those therapies are often ineffective. A more detailed understanding of the cerebral lipid imbalance and a novel therapeutic interventions are needed to halt the development of these diseases.

Here, we briefly reviewed the lipid composition in the cerebrovascular endothelium and its alteration under the disease condition. Furthermore, we discussed some of the potential therapeutic options and demonstrate the reason why we came up with the final nano-formulation.

1.1 Cerebrovascular endothelium

i. Overview of phospholipid species in the central nervous system (CNS)

The CNS is highly enriched in lipids that supports various key functions including providing energy and serving as important signaling molecules essential for brain accretion, synaptogenesis, and neurogenesis (Koundouros and Poulogiannis 2020). The major lipid species in the CNS are reported in the table below (**Table 1**). Among those lipids, phospholipids play a critical role in biological functions as structural components of cell membranes. Changes in composition of membrane phospholipids can lead to alteration of cell functions and cause metabolic or neurological diseases, such as type II diabetes (T2D) and Alzheimer's disease (AD). Major phospholipids in brain include phosphatidylcholine (PC), phosphatidylethanolamine (PE), phosphatidylethanolamine plasmalogen (PEpl), as well as smaller amounts of phosphatidylserine (PS), phosphatidylinositol (PI), and cardiolipin (CL). Fatty acids (FAs) are essential substrates of various lipids including phospholipids, sphingolipids, triglycerides, cholesterol ester, etc. Phospholipids have FAs that are structurally saturated [saturated FAs (SFAs)], contain one [monounsaturated FAs (MUFAs)] or more than one double bonds [polyunsaturated FAs (PUFAs)]. The common SFAs are palmitic acid (PAA, C16:0) and stearic acid (SA, C18:0) and MUFAs mainly includes oleic acids (OA, C18:1). PUFAs can be classified into two families according to the localization of the first double bond from the ω carbon terminal: ω-3 family, which include α-linolenic acid (ALA, C18:3), eicosapentaenoic acid (EPA, C20:5), and docosahexaenoic acid (DHA, C22:6); ω-6 family, which include linoleic acid (LA, C18:2), arachidonic acid (AA C20:4) and docosapentaenoic acid (DPA C22:5) (**Figure 1**). Moreover, based on the length of carbon tail, FAs can also be grouped as short (<6 carbons), medium (6-12 carbons), long (14-22 carbons), and very long (> 22 carbons) FAs (Fahy, Subramaniam et al. 2009, Cermenati, Mitro et al. 2015, Naudi, Cabre et al. 2015).

Category	Specific lipid species
Fatty acyls	Fatty acids, eicosanoids, endocannabinoids
Glycerolipids	DAGs, TAGs[a]
Glycerophospholipids	PC, PE, PEpl, PS, PI, CL[b]
Sphingolipids	Sulfatides, sphingomyelin, ceramides, ganglioside, glucosylceramide
Sterol lipids	Cholesterol

Table 1. Major lipid categories in the central nervous system

[a]DAGs: discyglycerols; TAGs: triacylglycerol; [b]PC: phosphatidylcholine; PE: phosphatidylethanolamine; PEpl: phosphatidylethanolamine plasmalogen; PS: phosphatidylserine; PI: phosphatidylinositol; CL: cardiolipin

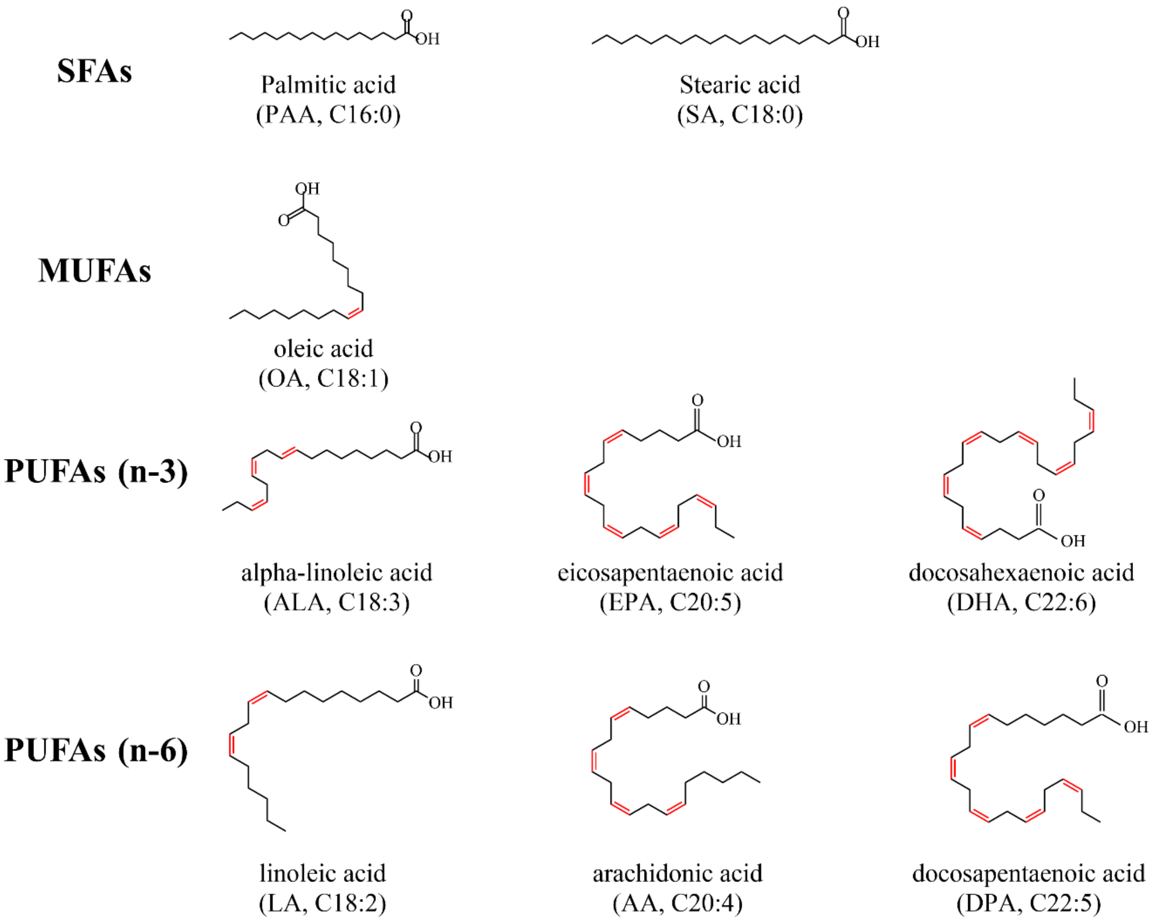

Figure 1. The chemical structure of major fatty acids

ii. Lipid transport at the blood-brain barrier (BBB)

The BBB endothelium lies at the blood-brain interface and conducts critical functions such as maintaining vascular response to regulate cerebral blood flow, transporting essential nutrients to sustain neuronal activity, and removing toxic metabolites from the brain. It is endowed with a battery of receptors/transporters, which is spatially orchestrated and precisely regulated by cell signaling networks (Andreone, Lacoste et al. 2015).

Although the brain is rich in lipids (containing 24% phospholipids, especially the long chain PUFAs), it has poor capability to synthesize lipids and therefore relies on being supplied from peripheral blood by transport across the BBB into the CNS (Svennerholm, Bostrom et al. 1997). The liver is the main site of synthesis of the long chain PUFAs including 20-carbon UFAs (such as EPA and AA) and 22-carbon UFAs (such as DHA and DPA) from ALA and LA by desaturation and elongation (Yamanaka, Clemans et al. 1980). The PUFAs can be released into the peripheral blood and supply other tissues including the brain. However, the essential PUFAs, such as α-linolenic acid (ALA, C18:3 ω-3) and linoleic acid (LA, C18:2 ω-3), cannot be synthesized *de novo* and must be dietary constituents because of the deficiency of enzymes, Δ-12, and Δ-15 desaturase, in the human beings (Zhang, Chen et al. 2018).

Lipids are transported across the BBB by one of three mechanisms (Pifferi, Laurent et al. 2021): (1) passive diffusion, (2) receptor-mediated transcytosis, and/or (3) transport via transmembrane proteins. Lipoproteins can be hydrolyzed by lipoprotein lipase enzymes within or outside the endothelial cells to produce free FAs and lysophospholipid (LPL). Free FAs in the plasma can associate with albumin and passively diffuse through the BBB or directly transport via transmembrane proteins, such as fatty acid transportation proteins (FATPs) (Edmond 2001), fatty acid translocase (FAT/CD36) (Mitchell, On et al.

2011), and major facilitator superfamily domain-containing protein (Mfsd2a) (Andreone, Chow et al. 2017). Once in the endothelial cells, FAs can bind to FA-binding proteins and shuttle through the cytosol, which will further transport into the brain either passively or via transmembrane proteins. Moreover, lipoprotein can bind to lipoprotein receptor and cross the BBB via transcytosis through either clathrin- or caveolae-coated vesicles (Brinkmann, Abumrad et al. 2002, Hamilton and Brunaldi 2007, Pan, Khalil et al. 2015, Zhang, Chen et al. 2018, Hachem, Belkouch et al. 2020) (**Figure 2**)

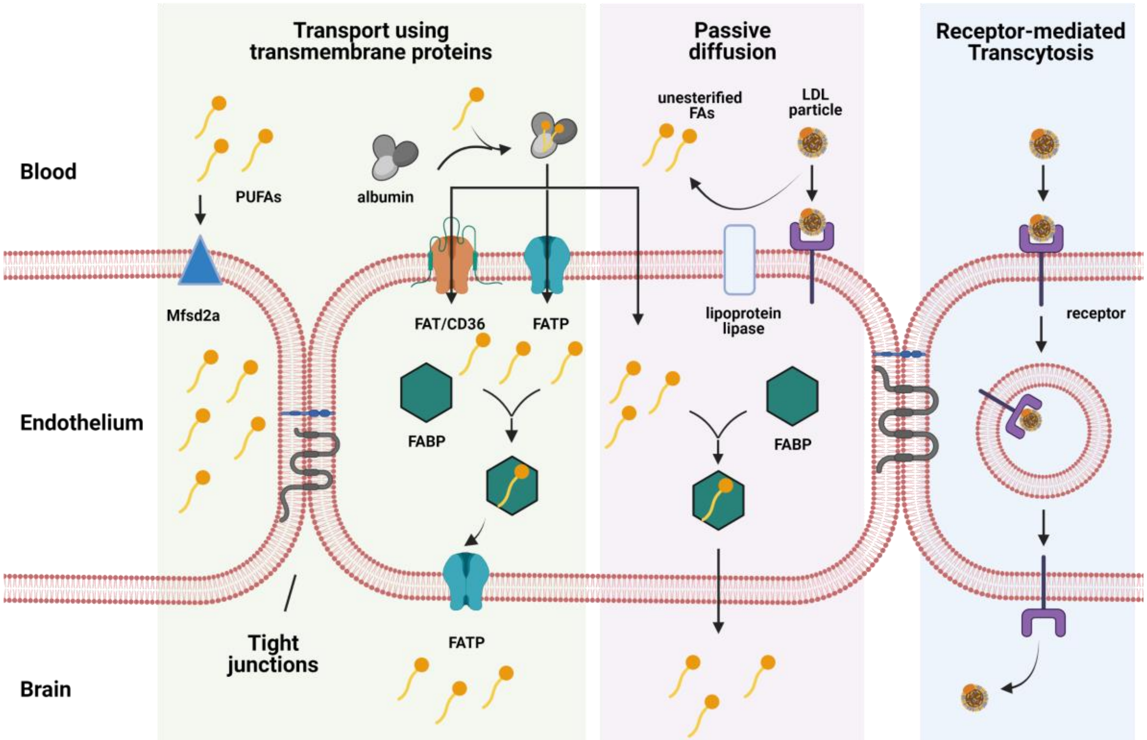

Figure 2. Lipid transport through the blood-brain barrier

iii. Unique lipid composition of CNS endothelium

Biological membranes are comprised of several phospholipid classes, which maintain membrane fluidity and function. The lipid composition varies greatly among different cell types. Brain endothelial cells has been reported that have approximately a three-fold higher amount of sphingomyelin and one-third lower amount of phosphatidylcholine compared with other endothelial cells (Siakotos and Rouser 1969, Takamura, Kasai et al. 1990, Campbell, Regina et al. 2014). In addition, Christine Benistant et al. (Benistant, Dehouck et al. 1995) investigated the fatty acid composition of brain capillary endothelial cells and found that it contains ~37.5% saturated fatty acids (SFAs) including palmitic acid (PAA, C16:0) and stearic acid (SA, C18:0), ~23.3 % monounsaturated fatty acids, and ~25.6 % PUFAs [mostly in the form of arachidonic acid (AA, C20:4 ω-6) and docosahexaenoic acid (DHA, C22:6 ω-3)]. The unique composition of the lipid domains present in brain endothelial cells regulates the restrictive trafficking and signal transduction at the BBB (Pike, Han et al. 2002, Vainio, Heino et al. 2002, Campbell, Regina et al. 2014). On one hand, it can markedly influence the passive permeability by alteration in phospholipid packing within the membrane and phospholipid-cholesterol interactions (Campbell, Regina et al. 2014). On the other hand, sphingolipid-cholesterol rich plasma membrane dynamic domains, known as lipid rafts, serve to regulate signal transduction and initiate signaling cascade (Pike, Han et al. 2002, Vainio, Heino et al. 2002). Lipid rafts involved in the transport of macromolecules, such as insulin, low-density lipoprotein (LDL), and high-density lipoproteins like apolipoprotein A-1 (ApoA-1), from plasma to the brain via the BBB. Moreover, insulin and other growth factor signaling, which is instrumental in maintaining the metabolic and mitogenic functions of the BBB, are also coordinated by the receptor tyrosine kinases in the lipid rafts (Filippini and D'Alessio , Pike 2003). Therefore, preserving the morphology of lipid rafts and maintaining unique composition of CNS endothelium are critical for the regulation of BBB integrity and function.

1.2 Brain lipids and lipid raft alteration in age-relevant diseases

Defective fatty acid homeostasis, especially PUFAs deficiency in the brain, is associated with age-relevant diseases. Metabolic diseases (Perona 2017, Cisa-Wieczorek and Hernandez-Alvarez 2020) are notable as are other neurodegenerative diseases, such as Alzheimer's disease (AD) (Chew, Solomon et al. 2020, Cisa-Wieczorek and Hernandez-Alvarez 2020).

i. Altered fatty acid uptake in the brain

Although increased brain fatty acids (FAs) uptake and accumulation is observed in obese subjects with metabolic syndrome (Karmi, Iozzo et al. 2010), the lack of PUFAs in the western diet can gradually cause a chronic pro-inflammatory status in the brain which later becomes one of the characteristics associated with neurodegenerative diseases (Zhang, Chen et al. 2018). Interestingly, long-term dietary deficiency of n-3 PUFAs just slightly changed the DHA (C22:6 ω-3) levels in neurons but significantly reduced the levels in other brain cells and organelles (such as astrocytes, oligodendrocytes, and myelin), which is consistent with the critical importance of preserving neuronal integrity. Neuronal membrane contains around 50% PUFAs despite their poor capacity to produce DHA (C22:6 ω-3) and AA (C20:4 ω-6) (Hooijmans and Kiliaan 2008). It is astrocytes and endothelial cells that play a significantly role in the brain via elongation and desaturation of essential FA precursors to PUFAs, which are then rapidly taken up by neurons and incorporated into their plasma membranes (Moore, Yoder et al. 1990, Moore, Yoder et al. 1991, Moore 1993). The endothelial cells mainly produce AA and EPA, while astrocytes predominantly produce DPA (C22:5 ω-6) and DHA. However, the free precursors of those PUFAs are not stable because they can undergo rapid ß-oxidized before they enter the brain, which makes PUFAs supplementation even more critical to maintain basic PUFA levels in the brain. Moreover, the recovery of ω-3 PUFAs levels in the brain was slower compared with the other peripheral organs after long-time dietary ω-3 DHA deficiency, which might be due to limited transport process through the BBB (Bourre, Durand et al. 1989, Connor, Neuringer et al. 1990, Moriguchi, Loewke et al. 2001).

In addition to dietary supplementation, aging and age-relevant diseases can also impact fatty acid uptake in the brain. Most of lipid species including phospholipids in the human brain have been shown to progressively decrease after 50 years old (Rouser and Yamamoto 1968, Farooqui, Liss et al. 1988, Naudi, Cabre et al. 2015). Several groups have demonstrated that the aging rodent brain tend to lose PUFAs (Delion, Chalon et al. 1997, Little, Lynch et al. 2007). In aging humans, DHA and AA were observed to decrease in the membrane of orbitofrontal cortex (McNamara, Liu et al. 2008, Hancock, Friedrich et al. 2015, Norris, Friedrich et al. 2015, Hancock, Friedrich et al. 2017). Age-related reduction in PUFA composition has also been shown to inversely correlate with elevated stearoyl-CoA desaturase expression and activity resulting in increasing production of MUFAs as a compensatory process (McNamara, Liu et al. 2008). Although the impact of aging on cerebral PUFAs uptake is not fully understood, there is increasing evidence showing alteration in specialized transport proteins at the BBB or reduction in enzymes activity regulating PUFAs synthesis in liver (Benistant, Dehouck et al. 1995, Pu, Igbavboa et al. 1999, Gao, Taha et al. 2013). FABPs are the proteins involved in FAs transport into the brain and their expression is decreased significantly in aged mouse brain (Pu, Igbavboa et al. 1999). The liver's capacity to synthesize PUFAs is reduced with aging as reported by Bourre and Piciotti (Bourre and Piciotti 1992). However, others also observed modified or unchanged hepatic desaturase activities in the aged rats (Bourre and Piciotti 1992, Bezard, Blond et al. 1994, Dinh, Bourre et al. 1995).

ii. Fatty acid-related alteration of membrane fluidity

The cell membranes are in the liquid crystalline state, which is characterized by considerable diffusive and conformational mobility in the two dimensions defining the plane of the cell membrane. The term, fluidity, is often used, which has its root in the measurement of the rotational motion of fluorescent probes associated with the membrane. Extensive studies in this field have shown that the fluidity is highly dependent on temperature, cholesterol levels, length of FAs, and degree of FA saturation (Maulucci, Cohen et al. 2016, Koundouros and Poulogiannis 2020). Higher temperature and shorter fatty acid chain lengths will increase membrane fluidity while higher cholesterol levels decrease the fluidity. The cell membrane exposed to saturated fatty acids (SFAs) is less fluid and less responsive to changes in the extracellular environment, while that exposed to unsaturated fatty acids (UFAs), such as PUFAs or MUFAs, confer a more dynamic microenvironment which can maintain membrane flexibility and fluidity (Hadders-Algra 2008, Maulucci, Cohen et al. 2016) as shown in **Figure 3**.

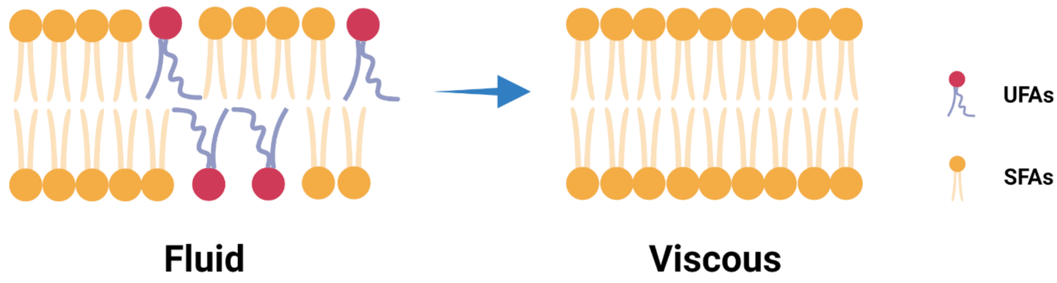

Figure 3. The saturation of fatty acids differentially regulates cell membrane fluidity.

Saturated fatty acids (SFAs) form viscous membrane (right), and unsaturated fatty acids (UFAs) forms fluid membrane (left).

iii. Altered lipid species and lipid rafts profile in the CNS

There is increasing evidence indicating an aberrant lipid raft profile is associated with aging-related diseases (Mesa-Herrera, Taoro-Gonzalez et al. 2019). Lipid rafts are membrane microdomains associated with cell signaling. The predominant fatty acid is palmitic acid (PAA, 16:0) while lower amounts of UFAs are present. The sphingolipids ganglioside (GM) is abundantly found in lipid rafts, and therefore commonly used as a lipid raft marker. In AD brains, both MUFAs and long chain PUFAs are reduced compared to normal brains (Martin, Fabelo et al. 2010), which alter lipid raft composition and thereby cause aberrant cell signaling, especially lipid raft regulated signaling. The highly ordered lipid rafts will induce amyloidogenic processing by recruiting more ß-secretase to cleavage amyloid protein precursor (APP), ultimately enhancing generation of Aß peptides, which is the main toxic protein causing AD (Mesa-Herrera, Taoro-Gonzalez et al. 2019) (Diaz, Fabelo et al. 2016).

Dyslipidemia prevalent in metabolic syndrome is also believed to disrupt lipid raft integrity. Elevation of ceramides can impair AKT expression and then disrupt insulin dependent glucose transport leading to risk of T2D (Perona 2017). Moreover, a close association between membrane lipid composition and insulin sensitivity has been observed in both animal models and humans. The elevated membrane viscosity was shown to impair the activation of the hepatic insulin receptor kinase in aging rats (Nadiv, Shinitzky et al. 1994). In addition, substitution of SFAs by MUFAs improved systemic insulin sensitivity in humans (Vessby, Uusitupa et al. 2001). Consistently, intracerebroventricular injections of oleic acids (OA, C18:1 ω-9) in Sprague-Dawley rats enhanced peripheral insulin sensitivity (Obici, Feng et al. 2002). Supplementation with ω-3 PUFAs also improved lipoprotein profile and insulin sensitivity in an insulin resistant mouse model (Lucero, Olano et al. 2017). Therefore, with aging, there is less PUFAs in the brain cell membranes, which decreases membrane fluidity and further attenuates its regulation on downstream signaling induction.

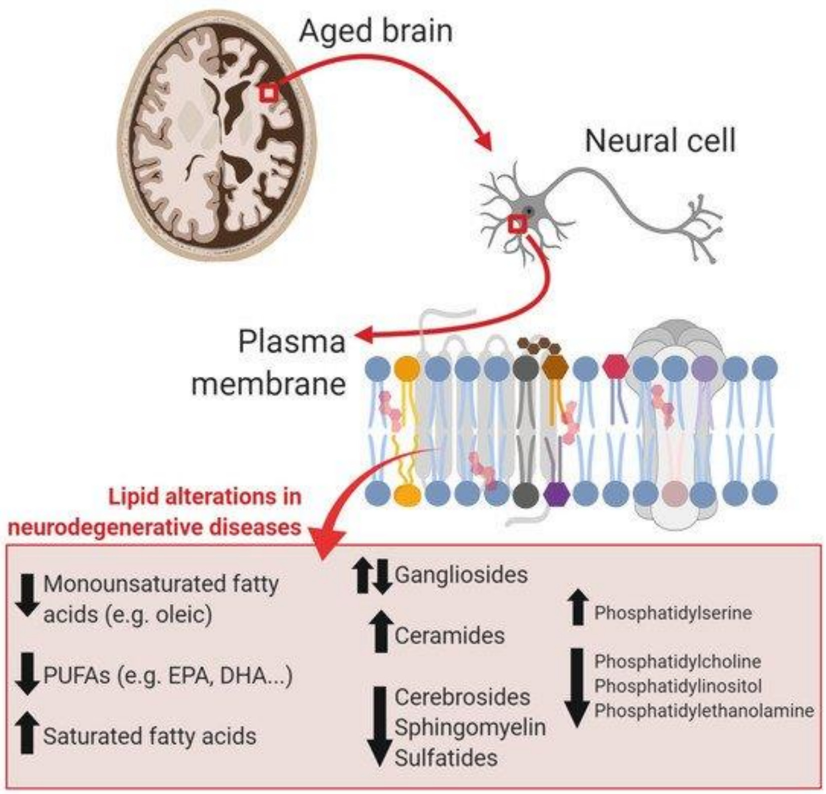

Figure 4. Schematic plot of lipid and lipid raft alteration in aging and neurodegenerative diseases (Mesa-Herrera, Taoro-Gonzalez et al. 2019)

1.3 Therapeutic options and limitations

Dietary supplementation with PUFAs such as EPA (20:5 ω-3) and DHA or intravenous administration of lipid emulsions has been widely used as common therapeutic options to improve the lipid composition in the brain cell membranes. However, the existing non-pharmacological treatments have moderate efficacy and higher risk of adverse effects. Administration of intravenous lipid emulsions results in an elevation of free fatty acid levels in the plasma, which triggers peripheral endothelial dysfunction (Steinberg, Paradisi et al. 2000, Umpierrez, Smiley et al. 2009, Gosmanov, Smiley et al. 2010, Gosmanov, Smiley et al. 2012). A chronic study has been conducted in rats with DHA dietary deficiency, which found a decrease of n-3 PUFAs in the liver and plasma, which are the main organs supplying lipids to the brain. Interestingly, the level of cerebral DHA did not return to normal after another eight weeks PUFAs feeding, indicating dietary supply is inefficient and can only cause minor changes in brain lipid composition (Moriguchi, Loewke et al. 2001).

1.4 Targeting nanoemulsions to the cerebrovasculature

The BBB is the critical boundary between neural tissue and circulating blood. Its unique and protective features control brain homeostasis as well as ion and molecular movement. Failure in maintaining any of these aspects results in the breakdown of the specialized multicellular structure and can lead to neuroinflammation and neurodegeneration. However, even a damaged and more permeable BBB can thwart drug delivery into the brain.

Currently, advances in the field of nanocarriers (including nanoemulsions, liposome, polymer nanoparticle, solid-lipid nanoparticle) have introduced several platforms that improve drug transport across the BBB. The structures of lipid-based nanocarriers are shown in **Figure 5**. Lipid-based nanocarriers can encapsulate therapeutically active drugs especially lipophilic drug and can be modified to target specific transport processes in the brain vasculature. This delivery platform can be used to enhance drug transport through the BBB in neurodegenerative/ischemic disorders and target relevant regions in the brain for regenerative processes. As such, these nanocarriers are considered one of the most promising and versatile drug delivery systems for reaching the brain. Moreover, nanocarriers can protect therapeutic agents in transit to the damaged areas (Ganta, Deshpande et al. 2010).

To modulate transport processes by altering the membrane composition, a particulate drug delivery system is needed that can both target the BBB and provide the required payload. To deliver unsaturated lipids to the BBB, it is perhaps self-evident that nanoemulsions would be superior. Nanoemulsions are dispersion of two immiscible liquids of lipid droplets and aqueous media with droplet sizes below 200 nm and mostly in the oil-in-water (O/W) form (Solè and Solans 2013). There are several advantages by using this nano-system. First, the oil core is a key formulation component for producing the desired nanoemulsions as well as the agent to achieve the change in the membrane composition. Polymeric and liposome- based systems can be ruled out, as they cannot achieve a payload level as nanoemulsions if we consider them as in the same droplet size. The choice of a nanoemulsion rather than solid lipid nanoparticles is driven by the nature of the lipids; that is, unsaturated lipids by using soybean oil or olive oil will be liquids at physiological temperatures. Second, nanoemulsions are inherently appealing from the perspective of product development, insofar as they are an equilibrium system. Due to their nano range droplet size, they present unique physicochemical characteristics with higher kinetic stability than conventional emulsions (Salvia-Trujillo, Soliva-Fortuny et al. 2017).

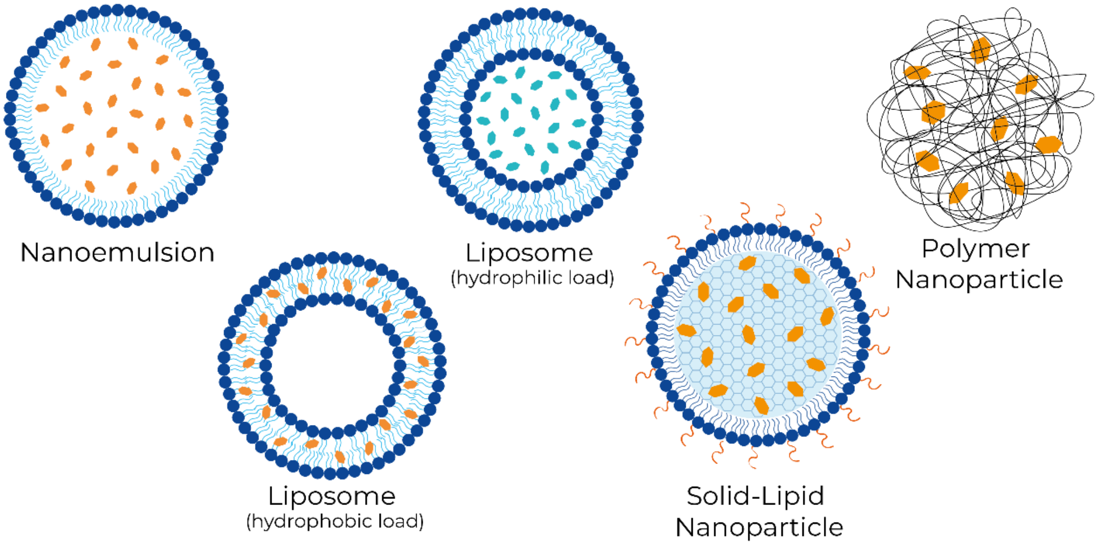

Figure 5. Common nanocarriers' structure (Melanie 2020)

1.5 Formulation of nanoemulsions

i. Structural components

Nanoemulsions have mainly three structural components including 1) active oil core, 2) surfactants, 3) various payloads that can be encapsulated for imaging or therapeutic functions (Ganta, Deshpande et al. 2010). Soybean oil and olive oil, which are composed of a large fraction of unsaturated lipids, were chosen as the appropriate lipid components in the oil core for correction of the underlying disease state. Surfactants were DOTAP (net positive charged) and DMPC (zwitterionic) or DPPC (zwitterionic) (**Figure 6**), which allows preparation of stable nanoemulsions that vary in size and zeta potential without creaming or phase separation (Vyas, Shahiwala et al. 2008). To further characterize nanoemulsions' therapeutic impact on insulin trafficking and signaling, we used the fluorescent compound, 1,1'dioctadecyl-3,3,3',3'-tetramethyl indocarbocyanine (DiI-C18) incorporated into the phase of bioactive oil in the nanoemulsions.

ii. Formation method

Nanoemulsions can be formed by using high-energy or low energy methods. High-energy methods (Aksoylu Özbek, Günç Ergönül et al. 2020) usually reduce the droplet sizes by intense mechanical force through ultrasonic waves, stirring, shearing, or cavitation. In contrast, low-energy methods (Aboudzadeh and Hamzehlou 2020) only require a low quantity of energy by using spontaneous emulsification (SE) or emulsion phase inversion (EPI) as show in the **Figure 7**. Oils with long chain triglycerides that we used can form larger oil droplets because of the lipid phase viscosity (Qian and McClements 2011). Therefore, we chose to use high-energy method to formulate the nanoemulsions as this method can effectively reduce the size of droplet and can be eventually applied in the industry (Kumar, Bishnoi et al. 2019).

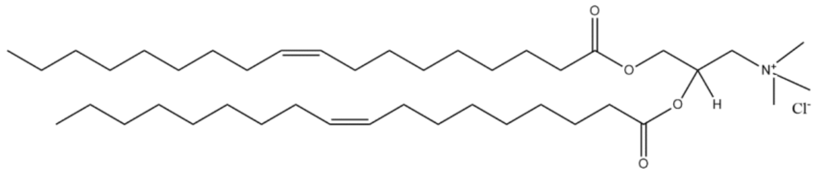

1,2-dioleoyl-3-trimethylammonium-propane (DOTAP) as a chloride salt

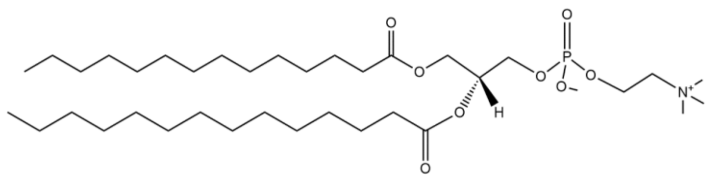

Dimyristoylphosphatidylcholine (DMPC)

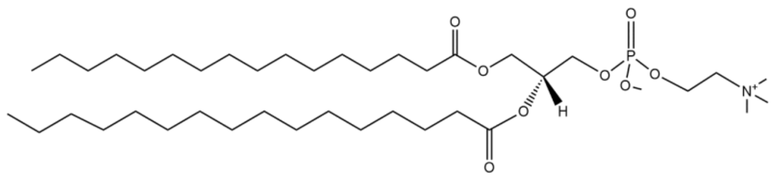

1,2-dipalmitoyl-sn-glycero-3-phosphocholine (DPPC)

Figure 6. Chemical structures of surfactants used in lipid based nanoemulsion formulations

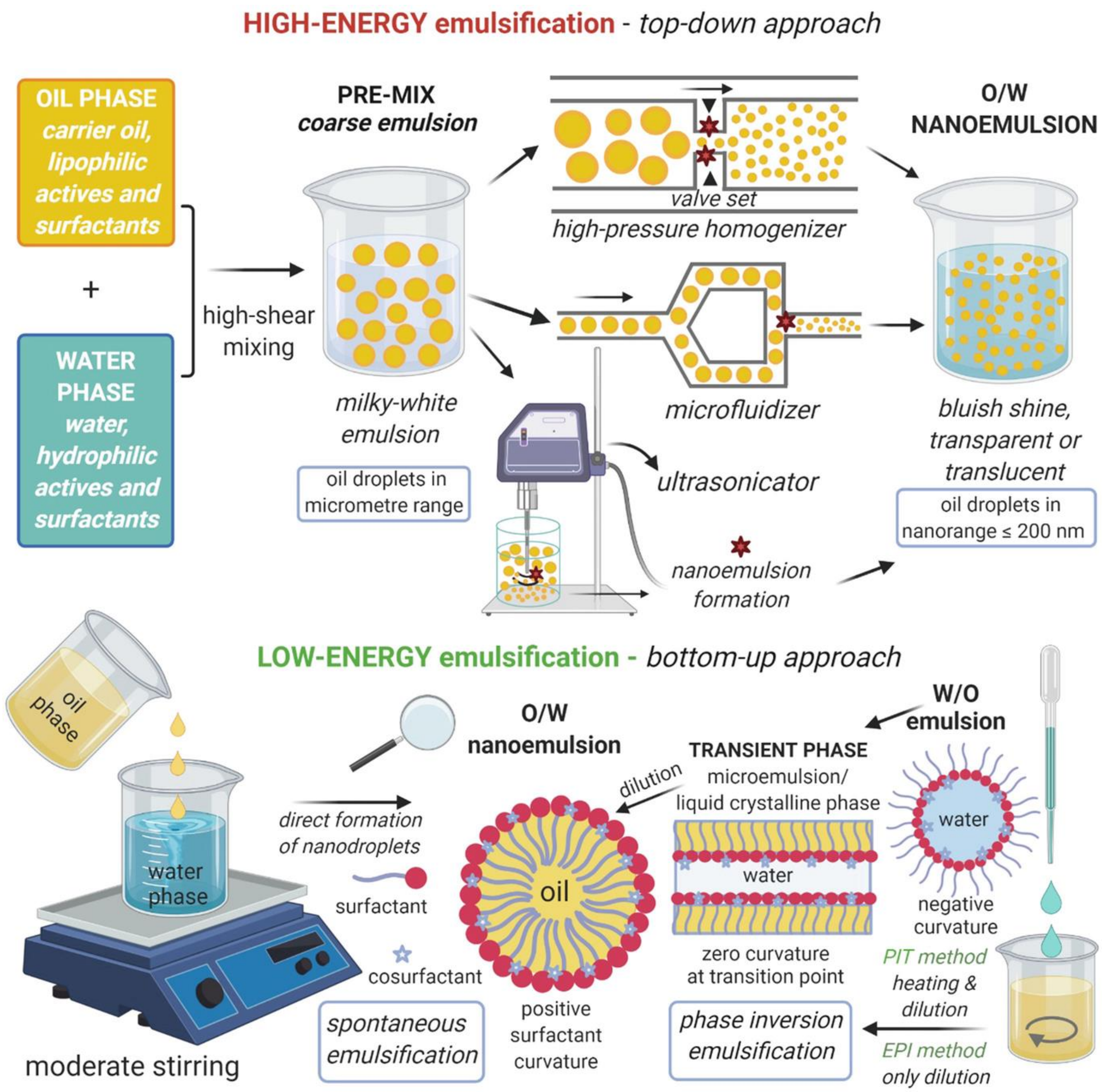

Figure 7. Schematic representation of O/W nanoemulsions formation through high-energy and low-energy emulsification methods (Nikolić, Gledović et al. 2020)

iii. Membrane filter extrusion

The extruder filter assembly with uniform pores is an attractive approach to reduce nanoemulsions size within the desired size range. In the extrusion process, the dispersion is passed several times through the pores of a membrane, which can yield a smaller droplet size. This technique with porous membranes is a variation of the direct membrane emulsification process. The energy density during premix membrane emulsification is much lower than during high-pressure homogenization. An advantage of membrane emulsification techniques is the possibility to prepare monodisperse particle size distributions of the products, which is highly desirable for pharmaceutical formulations **(Figure 8)**.

iv. Zeta potential

The zeta potential is a common method to measure the surface charge of particles dispersed in liquid. It is one of the critical parameters regarding stability of the nano-system and permeation properties through the BBB. The choice of high positive zeta potential rather than high negative zeta potential is due to the consideration of efficient brain delivery. Because a positively charged nanoemulsions could interact with the negatively charged cell membrane by electrostatic attraction and further results in efficient uptake (**Figure 9**) (Voigt, Christensen et al. 2014).

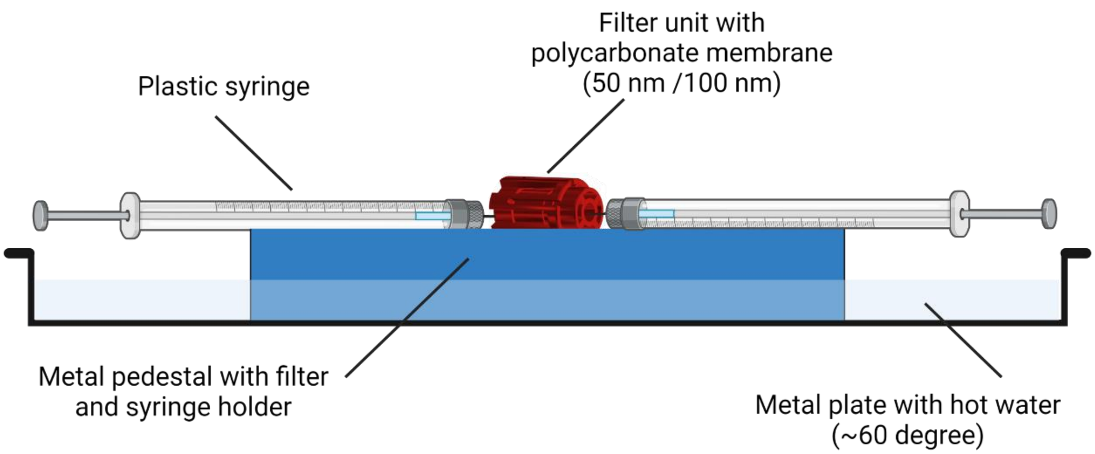

Figure 8. Nanoemulsions extrusion tools

The metal plate was filled with hot water around 60 degrees. Two syringes and membrane filter unit of selected pore size was set up on the metal pedestal. One syringe is filled with the nanoemulsion solution, which is extruded 20 times from one syringe to the other through the 100 nm membrane filter and then through the 50 nm filter, to create small nanosized emulsions.

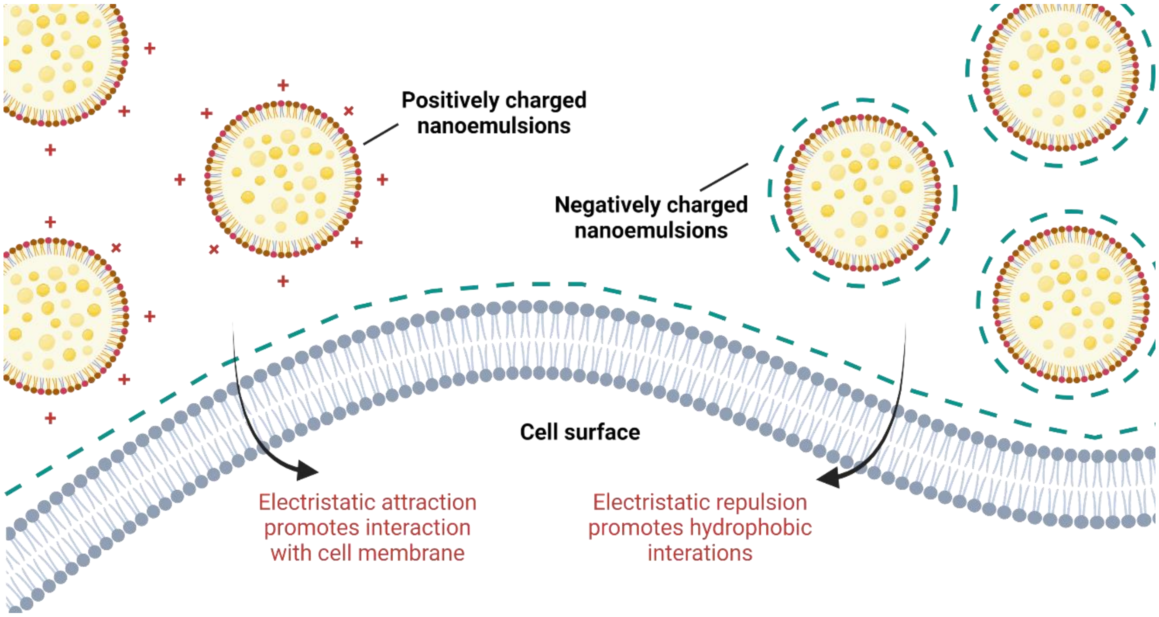

Figure 9. Schematic plot of the electrostatic interactions between nanoemulsions and negatively charged cell surface

1.6 Hypothesis

The working hypothesis of this thesis was: the delivery of nanoemulsions containing unsaturated lipids will favorably alter the membrane lipid composition and correct the aberrant trafficking/ signaling of insulin.

1.7 Specific aims

The specific aims of this thesis are as follows:

Specific aim1: Formulate, optimize, and characterize lipid-based nanoemulsions for cerebrovascular delivery.

Specific aim2: Evaluate the impact of lipid-based nanoemulsions encapsulated with unsaturated lipids on insulin trafficking and signaling function.

Specific aim3: Investigate the impact of lipid-based nanoemulsions encapsulated with unsaturated lipids on lipid rafts integrity.

1.8 Scientific rationale

In this study, we evaluated the impact of fatty acid exposure on one of the important receptors located in the lipid rafts, the insulin receptor, which regulates vital BBB functions. Dietary oils that consist of a variety of these fatty acids, such as soybean and olive oil, are formulated as lipid based nanoemulsions. Soybean oil is abundant in ω-6 PUFAs while olive oil has ~85% of nonessential oleic acids, ω-9 MUFAs (Gramlich, Ireton-Jones et al. 2019). Both these oils are widely used in intravenous lipid emulsions administered to treat fatty acid deficiency (Dai, Sun et al. 2016) (Swaminathan, Ahlschwede et al. 2018). The effect of these nanoemulsions on insulin trafficking/signaling, whose impairment is implicated in brain insulin resistance, were investigated in the current study.

2. Materials and methods

The phosphatidylcholines, 1, 2-dimyristoyl-sn-glycero-3-phosphatidylcholine (DMPC) and 1,2-dipalmitoyl-sn-glycero-3-phosphocholine (DPPC), and 1,2-dioleoyl-3-trimethylammonium-propane as a chloride salt (DOTAP) were purchased from Avanti Polar Lipids, Inc. (Alabaster, AL). Soybean and olive oil were purchased from Sigma-Aldrich (St. Louis, MO). The fluorescent compound, 1, 1'dioctadecyl-3, 3, 3', 3'-tetramethyl indocarbocyanine (DiI-C18), was purchased from Frontier Chemical (Boulder, CO). Human basic fibroblast growth factor (bFGF) was purchased from PeproTech (Rocky Hill, USA). Fetal bovine serum (FBS) was purchased from Atlanta Biologics (Flowery Branch, GA). Dulbecco's phosphate buffered saline (DPBS, 1X) was purchased by Mediatech (Manassas, VA). All other chemicals were analytical grade.

2.1 Nanoemulsion preparation

Dispersions of lipids in normal saline solution [0.9% sodium chloride (NaCl) in water] were prepared on a weight basis. Pyrex screw cap test tubes were weighed, and water-insoluble surfactants, DMPC/DPPC and DOTAP, were added by weight from stock solutions of chloroform. For (DOTAP: DMPC) and (DOTAP: DPPC) SNEs, the weight ratios of DOTAP to DMPC or DOTAP to DPPC were 9:1, 7:1 or 3:1. The surfactants were dried as a thin film under nitrogen gas, the residual solvent is removed under vacuum and the dry weight was then measured. Then, DiIC18 was incorporated into the SNEs by adding 100 μL of DiIC18 (1 mg/mL) in soybean oil to the dried thin film in the test tubes followed by vortex mixing. Then, 5 mL of normal saline solution was added, and the sample was vortexed until a visibly uniform dispersion was obtained. The samples were then stored overnight in the refrigerator. Approximately 0.6 mL of the resultant lipid dispersion was then drawn into a 1 mL syringe and extruded through the pores of a single clean, track-etched polycarbonate membrane (pore size 50, 100 nm) positioned in a small-volume extruder (NanoSizerTM Mini Extruder; T&T Scientific Corporation, Knoxville, TN). The dispersion was pre-extruded 21 cycles with a 100 nm membrane and then for 21 cycles with the 50 nm membrane. The ONEs (DOTAP: DPPC) were made using the same method described previously with weight ratios of 3:1, 3:2, or 1:1. All nanoemulsion formulations were thoroughly characterized and were stored at 4 °C **(Figure 8)**. Only SNEs [DOTAP: DMPC (7:1 w/w)], SNEs [DOTAP: DPPC (7:1 w/w)], and ONEs [DOTAP: DPPC (3:1 w/w)] were used for in vitro studies.

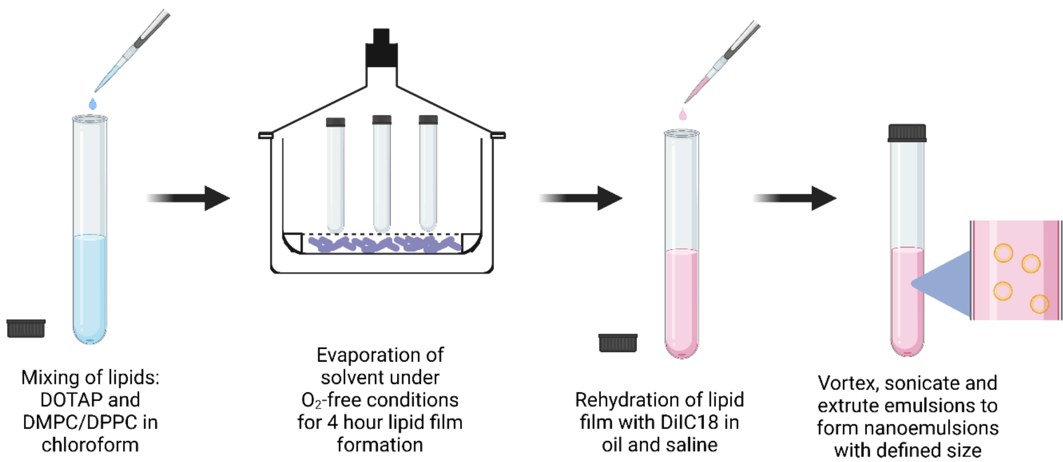

Figure 10. Schematic diagram of nanoemulsion preparation

2.2 Nanoemulsion characterization

Nanoparticle tracking analysis. Size measurements of nanoemulsions were carried out using NanoSight LM-10 Model (Malvern Instruments Ltd., Malvern, UK) configured with a temperature controller and is equipped with a 405 nm laser (near UV) inside the flow cell. The tracking of the Brownian motion of individual particles was recorded by the sCMOS camera at 30 frames/sec. The video images of moving particles were captured and analyzed by the nanoparticle tracking 2.3 image analysis software (NanoSight, USA) to assess the displacement of the particle in the x-y plane. The displacement is then used to estimate the diffusion coefficient, from which the hydrodynamic diameter was calculated using the Stokes-Einstein equation. Three measurements were conducted for each sample. The mean, mode, and distribution standard deviation values were determined based on the particle sizes analyzed by the software. The mean and standard deviation of the number particles per mL were also determined.

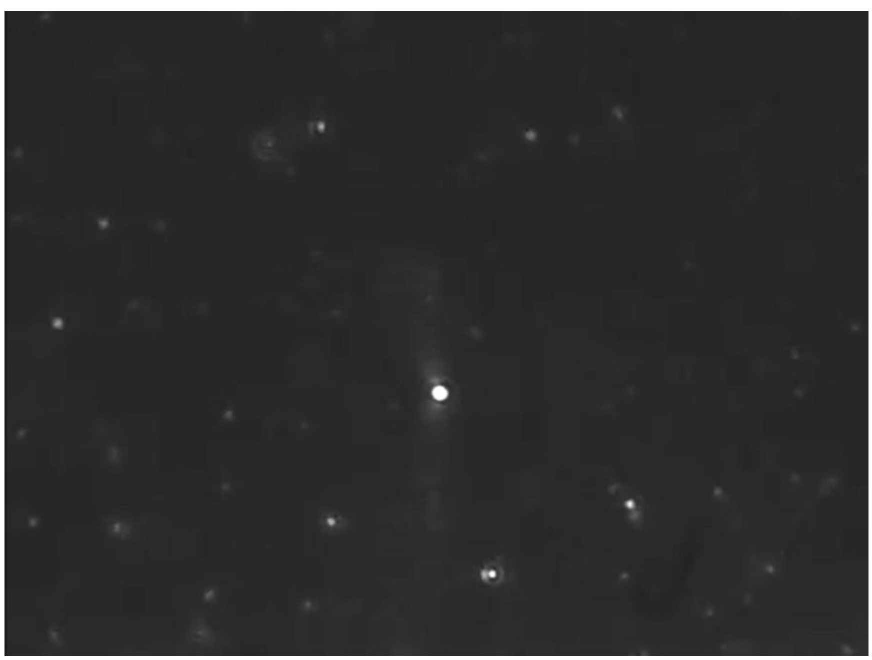

Figure 11. Videa snapshot of SNEs (DOTAP: DMPC, 7:1 w/w)

Zeta potential analysis. The zeta potential was measured by Delsa Nano (Beckman Coulter, Inc., Brea, CA). Single measurements were made based on 70 accumulated scans captured at refractive index, 1.33; viscosity, 0.89 cP; dielectric constant, 78.3; and temperature, 25 °C.

2.3 Cell culture

Human cerebral microvascular endothelial cell line (hCMEC/D3), a kind gift from P-O. Couraud (Institute Cochin, France), was used as the BBB model in vitro. The cells were cultured at 37°C and 5% CO_2 in endothelial cell basal medium (Sigma-Aldrich, St. Louis, MO), supplemented with 5% v/v FBS.

2.4 Flow cytometry

Cell and insulin uptake measurements. For cellular uptake measurements, the hCMEC/D3 cells incubated at various concentrations (0, 2, 5, 10, 20, 60/90 µg/mL) of SNEs [DOTAP: DMPC (7:1 w/w), DOTAP: DPPC (7:1 w/w)], or ONEs [DOTAP: DPPC (3:1 w/w)] laced with the fluorophore DiIC18. One hour following the incubation, the cells were washed with ice-cold DPBS, removed from the substrate by gentle trypsinization, suspended in ice-cold DPBS, and the intracellular fluorescence was captured by LSR-II Fortessa flow cytometer (BD Biosciences, San Jose, CA) equipped with 561 nm laser and 585/15 band-pass filter. The results were analyzed using FlowJo software (TreeStar Inc., San Carlos, CA). For the insulin uptake measurements, the hCMEC/D3 cells were first incubated with 60 µg/mL SNEs [DOTAP: DMPC (7:1 w/w)], SNEs [DOTAP: DPPC (7:1 w/w)] or ONEs [DOTAP: DPPC (3:1 w/w)] for 1 hour following with or without Alexa Fluor 647-labeled insulin (AF647-insulin; 200 nM, 20 min) stimulation. The cells were then washed, trypsinized, resuspended, measured intracellular AF647-insulin fluorescence intensity as mentioned above.

2.5 Western blot

After treatment with the nanoemulsions (0, 20, 60 µg/mL, 1 hour) followed by insulin stimulation (100 nM, 20 min), the hCMEC/D3 cells were washed with ice-cold Dulbecco's PBS, dislodged from tissue culture dishes using a cell scraper. To the cell suspension, 50 uL of radio-immunoprecipitation assay (RIPA) buffer (Thermo Scientific, Waltham, MA) containing EDTA-free protease inhibitor cocktail (Roche, Branford, CT) and phosphatase (Roche, Branford, CT) inhibitors were added. The cell lysates thus obtained were centrifuged at 10,000 rpm for 10 min at 4 °C and the protein concentration was determined using the bicinchoninic acid (BCA) assay (Pierce, Rockford, IL). Expression of Akt, p-Akt, and GAPDH in the cell lysates was assessed by western blots. Density of the western blots was quantified using Image J software (National Institute of Mental Health, Bethesda, Maryland). The differences among different treatments were statistically analyzed using GraphPad Prism software (La Jolla, CA).

2.6 Confocal microscopy

The hCMEC/D3 cells were cultured on 12 mm Transwell® filters (corning) as described in our previous publication (Swaminathan, Ahlschwede et al. 2018). Luminal side of the polarized monolayers of hCMEC/D3 cells were pre-incubated with 60 µg/mL SNEs [DOTAP: DMPC (7:1 w/w), DOTAP: DPPC (7:1 w/w)] or ONEs [DOTAP: DPPC (3:1 w/w)] in 500 µL of Dulbecco's modified Eagle's Medium (DMEM, without phenol red) for 1 hour at 37 °C. The hCMEC/D3 monolayer was washed 3 times with DPBS and fixed in 500 µL ice-cold 4% v/v PFA for 1 hour. The fixed cells were then washed 3 times with DPBS and mounted with ProLong Diamond Mounting medium containing DAPI (Invitrogen, Carlsbad, CA), a nuclear stain. At the end of the experiment, the Transwell® filter was mounted on a glass coverslip and imaged using Zeiss LSM 780 laser confocal microscope equipped with a C-Apochromat 40x/1.2W objective.

2.7 Effect of nanoemulsions on the integrity of lipid rafts

The hCMEC/D3 cell monolayers cultured on 35-mm coverslip bottom dishes were pretreated with medium alone, 60 µg/mL of SNEs [DOTAP: DMPC (7:1 w/w) or DOTAP: DPPC (7:1 w/w)], or ONEs [DOTAP: DPPC (3:1 w/w)] in cell culture medium at 37 °C. Then the cells were washed with DPBS and then incubated with 5 µg/mL of AF647 conjugated Cholera Toxin Subunit B (AF647-CXT; Thermo Scientific, Waltham, MA) for another 30 minutes at 37 °C. The cell monolayers were then washed, fixed, mounted, and imaged by confocal microscopy as mentioned above.

2.8 Data analysis

The volume of encapsulated oil, V_{oil} in the nanoemulsions was determined as described below:

$$V_{oil} = \frac{1}{6}\pi d^3$$

Where d is the diameter (mode) of the nanoemulsion particles determined by Nanoparticle Tracking Analysis.

Given the volume of encapsulated oil in each nanoemulsion, the nanoemulsion concentration (µg/mL) in each well of 6-well plates was determined as follows:

$$\text{Concentration of nanoemulsions} = \frac{V_n * V_{oil} * \rho * N}{1.5\ \text{mL}}$$

where 1.5 mL is the volume of DMEM (w/o phenol red) used in each well, ρ is density of oil (g/mL) as reported by the manufacturer (soybean oil: 0.917 g/mL; olive oil: 0.9087 g/mL), N is number of nanoemulsions per mL, obtained from Nanoparticle Tracking Analysis summary, and V_n is the volume (µL) of nanoemulsion suspensions added into each well.

2.9 Statistical analysis

All statistical tests were conducted using GraphPad Prism (GraphPad Software, La Jolla, CA). The statistical significance of difference in the median fluorescence intensity of insulin uptake, phosphorylation of AKT in cells treated with/without nanoemulsions, and the effect of nanoemulsions on lipid rafts labelled by AF647-CXT were evaluated by one-way ANOVA followed by Bonferroni post-tests.

3. Results

3.1 Preparation and characterization of nanoemulsions

Lipid based nanoemulsions were prepared by the desolvation technique previously described (von Corswant and Söderman 1998, Flanagan, Kortegaard et al. 2006, Bhattacharjee 2016). The surfactants, DMPC/DPPC and DOTAP, were cast as a thin film in a glass test tube and then dispersed in soybean or olive oil. The preparation had a distinctly white appearance indicative of particles with size at or above the wavelength of visible light. Extrusion through membrane filters of 100 nm and then 50 nm resulted in a reduction of particle size as determined by nanoparticle tracking analysis, confirming the reduction in nanoemulsion size. As summarized in **Table 2**, the size of SNEs [DOTAP: DMPC (9:1 w/w)] was 149 ± 110 nm and the sizes of 7:1 and 3:1 (w/w) (DOTAP: DMPC) SNEs were 132 ± 91 nm and 130 ± 120, respectively. The zeta potentials of the nanoemulsions were all positive. Similar size ranges were observed with SNEs made by DOTAP and DPPC where the 7:1 w/w formulation was 145 ± 78.5 nm **(Table 3)**. In case of ONEs, the size of 3:1 w/w (DOTAP: DPPC) formulation was 171 ± 80 nm, whereas for the ratios of 3:2 and 1:1 w/w (DOTAP: DPPC) ONEs, the sizes were found to be 181 ± 117 and 178 ± 108 nm, respectively **(Table 4)**.

Table 2. Composition and characterization of soybean oil nanoemulsions fabricated with DOTAP and DMPC.

Nominal Composition[a]	Mole fraction DOTAP[b]	Surfactant/soy oil weight ratio	Hydrodynamic diameter, nm (NT[C])	Zeta Potential, mV
9:1	0.90	0.13	149 ± 110	61
7:1	0.84	0.15	132 ± 91	62
3:1	0.72	0.18	130 ± 120	62

[a]Nominal composition by weight DOTAP: DMPC
[b]Surfactant mixture contains DOTAP and DMPC
[C]Nanotracker: <mode>ave

Table 3. Composition and characterization of soybean oil nanoemulsions fabricated with DOTAP and DPPC.

Nominal Composition[a]	Mole fraction DOTAP[b]	Surfactant/soy oil weight ratio	Hydrodynamic diameter, nm (NT[C])	Zeta Potential, mV
9:1	0.89	0.19	164 ± 101	59
7:1	0.86	0.26	145 ± 78.5	60
3:1	0.73	0.22	115 ± 53	67
1:1	0.46	0.22	175± 70.6	67
1:3	0.23	0.22	100± 17.6	74

[a]Nominal composition by weight DOTAP: DPPC
[b]Surfactant mixture contains DOTAP and DPPC
[C]Nanotracker: <mode>ave

Table 4. Composition and characterization of olive oil nanoemulsions fabricated with DOTAP and DPPC.

Nominal Composition[a]	Mole fraction DOTAP[b]	Surfactant/olive oil weight ratio	Hydrodynamic diameter, nm (NT[C])	Zeta Potential , mV
3:1	0.80	0.28	171 ± 80	60
3:2	0.58	0.37	181 ± 117	61
1:1	0.45	0.31	178± 108	62

[a]Nominal composition by weight DOTAP: DPPC
[b]Surfactant mixture contains DOTAP and DPPC
[C]Nanotracker: <mode>ave

3.2 Cellular uptake of diI-nanoemulsions in hCMEC/D3 cells by fow cytometry

The endothelial uptake of the SNEs formulated with 7:1 (w/w) DOTAP: DMPC/DPPC or ONEs formulated with 3:1 (w/w) DOTAP: DPPC was assessed by flow cytometry. As seen in **Figure 11 A**, about 58.0% of hCMEC/D3 cells incubated with 5 µg/mL of SNEs [DOTAP: DMPC (7:1 w/w)] internalized the SNEs, and at the concentration of 10 µg/mL, almost all the cells internalized SNEs. Similar pattern was observed when hCMEC/D3 cells were incubated with 60 µg/mL of SNEs or ONEs fabricated with DPPC, where 99.7% and 97.1% of cells internalized SNEs [DOTAP: DPPC (7:1 w/w)] and ONEs [DOTAP: DPPC (3:1 w/w)], respectively **(Figure 11 B&C)**.

3.3 Trafficking of diI-nanoemulsions at the BBB endothelium

The z-stack micrographs of polarized hCMEC/D3 endothelial cell monolayers incubated with 60 µg/mL of DiI-labelled SNEs [DOTAP: DMPC (7:1 w/w); **Figure 12 A**], SNEs [DOTAP: DPPC (7:1 w/w); **Figure 12 B**], or ONEs [DOTAP: DPPC (3:1 w/w); **Figure 12 C**] on the luminal (blood) side showed internalization by the endothelial cells**.** Upon closer examination of the micrographs in x-z (horizontal), and y-z (vertical) planes, tracts of DiI-labeled nanoemulsions in transit to the abluminal (brain) side of the endothelium were clearly evident **(Figure 12 D)**.

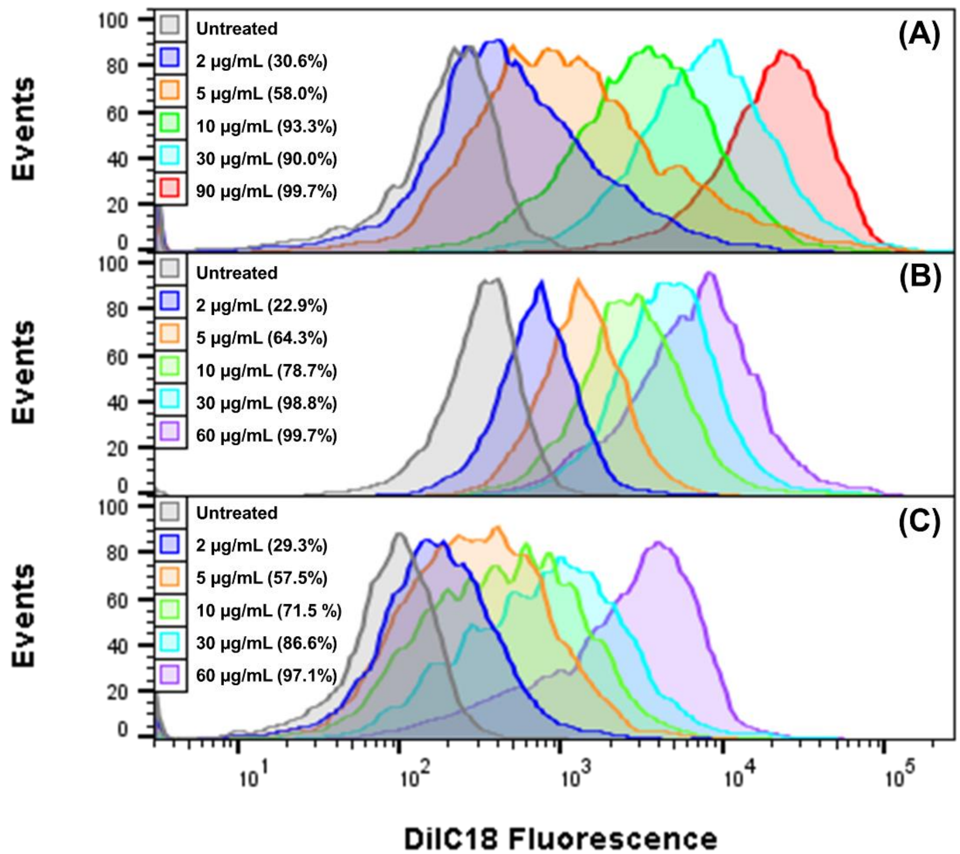

Figure 12. Concentration-dependent nanoemulsion uptake in hCMEC/D3 monolayer

Representative flow cytometry histograms showing similar dose-dependent increase in the hCMEC/D3 cell uptake of DiI561-nanoemulsions after 1-hour treatment. **(A)** SNEs formulated with DOTAP: DMPC (7:1 w/w). **(B)** SNEs formulated with DOTAP: DPPC (7:1 w/w). **(C)** ONEs formulated with DOTAP: DPPC (3:1 w/w).

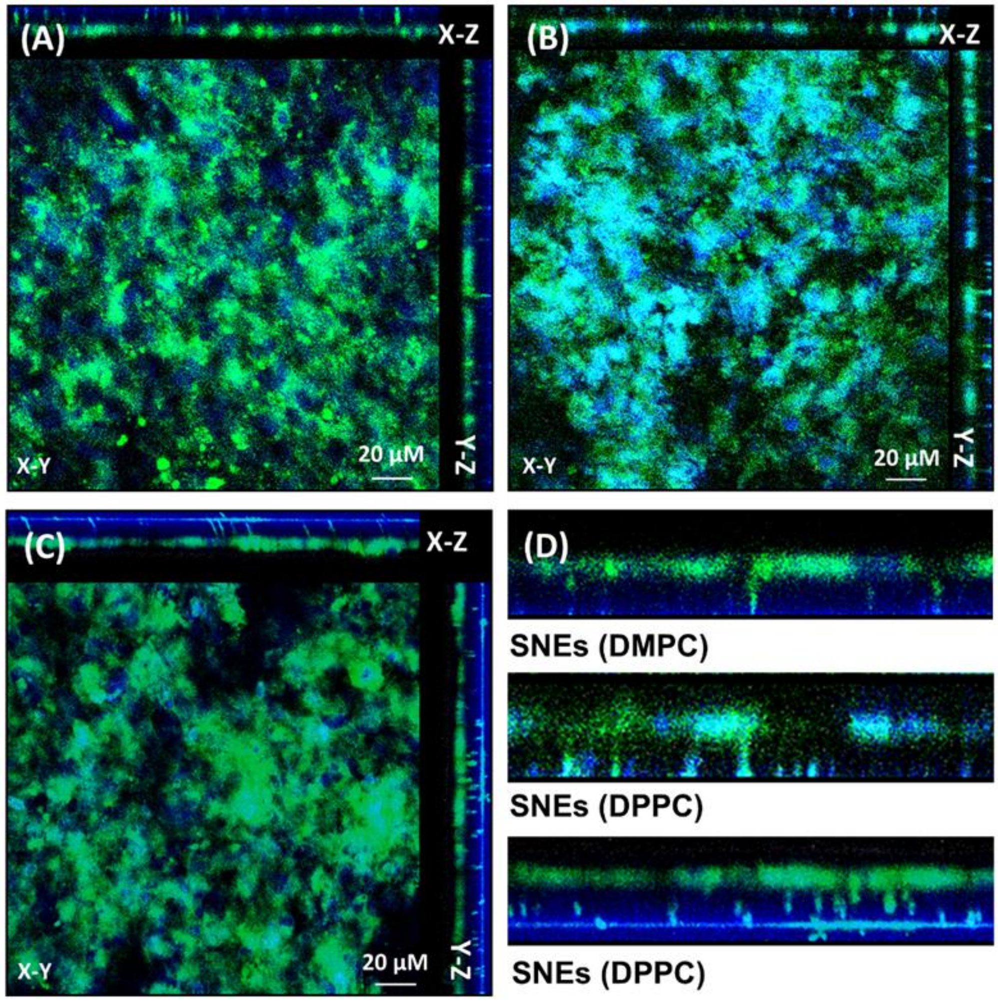

Figure 13. Transcytosis of DiI-nanoemulsions across hCMEC/D3 monolayers cultured on 0.4 µM Transwell filters

The Z-stack composite image demonstrated internalization of DiI-SNEs [DOTAP: DMPC (7:1 w/w)**; A**], DiI-SNEs [DOTAP: DPPC (7:1 w/w); **B**], and DiI-ONEs [DOTAP: DPPC (3:1 w/w); **C**] in polarized hCMEC/D3 monolayers after 1 hour incubation on the luminal side. The image presented in X-Y (transversal), X-Z (vertical), and Y-Z (vertical) planes was constructed from 32 optical sections imaged with a composite of 32 optical sections imaged with a 0.53 µm Z-step interval. **(D)** Enlarged section of the Y-Z plane showing cellular uptake of DiI-nanoemulsions across the endothelium. Green = DiI-nanoemulsions; Blue = DAPI-stained nuclei.

3.4 Effect of nanoemulsions on insulin uptake in hCMEC/D3 cells

The uptake of AF647-insulin by hCMEC/D3 monolayers with and without pretreatment with nanoemulsions was investigated. As assessed by flow cytometry, the AF647-insulin uptake increased by 2 to 3-fold in hCMEC/D3 monolayers pretreated with SNEs [DOTAP: DMPC (7:1 w/w) and DOTAP: DPPC (7:1 w/w)] compared to control cells **(Figure 13 A, B, D, E)**. However, no significant change in AF647-insulin uptake was found in ONEs [DOTAP: DPPC (3:1 w/w)] pre-treated cells **(Figure 13 C&F)**.

3.5 Effect of nanoemulsions on insulin signaling in hCMEC/D3 cells

The western blot analysis **(Figure 14 A, B & C)** showed a significant increase in AKT phosphorylation in the hCMEC/D3 cells treated with both SNEs [DOTAP: DMPC (7:1 w/w); 60 µg/mL] and SNEs [DOTAP: DPPC (7:1 w/w); 60 µg/mL]. Densitometric analysis of the bands showed that SNEs increased p-AKT expression by 2-fold compared to the control. No significant change in the p-AKT expression was observed between the control and ONE [DOTAP: DPPC (3:1 w/w); 60 µg/mL] pre-treated cells **(Figure 14 D)**.

3.6 Effect of nanoemulsions on lipid rafts in hCMEC/D3 cells

The uptake of AF647-CXT by hCMEC/D3 monolayers with and without pretreatment with nanoemulsions was investigated by microscopy to evaluate the effect of nanoemulsions on lipid rafts. The cholera toxin subunit B was widely used to label lipid rafts (Day and Kenworthy 2015). As a result, both SNEs [DOTAP: DMPC (7:1 w/w; **Figure 15 C**) or DOTAP: DPPC (7:1 w/w; **Figure 15 D**)] significantly reduced the labeling of cells by AF647-CXT compared to the cells treated with AF647-CXT alone (**Figure 15 B**). In addition, ONEs [DOTAP: DPPC (3:1 w/w; **Figure 15 E**)] did not significantly alter the labeling of hCMEC/D3 cell monolayers by AF647-CXT.

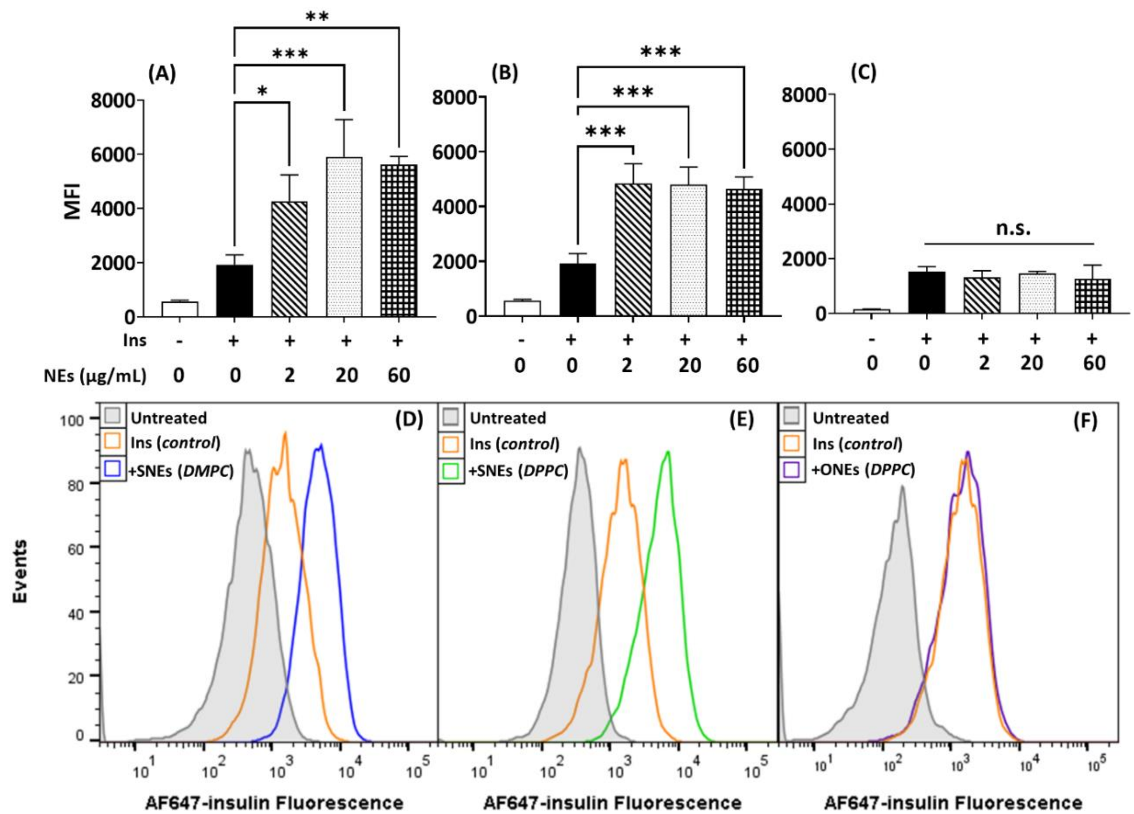

Figure 14. SNEs increased insulin uptake in hCMEC/D3 monolayers.

Flow cytometry was used to evaluate dose-dependent AlexaFluor-647 labelled insulin (AF647-insulin) uptake after pretreatment with SNEs [DOTAP: DMPC (7:1 w/w); **A**], SNEs [DOTAP: DPPC (7:1 w/w); **B**], ONEs [DOTAP: DPPC (3:1 w/w); **C**] following with or without AF647-insulin (200 nM, 20 min) treatment. Bar chart of median fluorescence intensity (MFI) of AF647-insulin showed increased insulin uptake in the SNEs pretreated cells compared with cells treated with AF647-insulin alone (MFI ± SD; n=3). Representative flow cytometry histograms showing an increase in the fluorescence uptake of AF647-insulin after 1 hour of pretreatment with SNEs [DOTAP: DMPC (7:1 w/w); **D**] and SNEs [DOTAP: DPPC (7:1 w/w); **E**], but there is no significant difference in ONEs [DOTAP: DPPC (3:1 w/w); **F**] (One-way ANOVA with Bonferroni post-tests, *P<0.05, ***p<0.005).

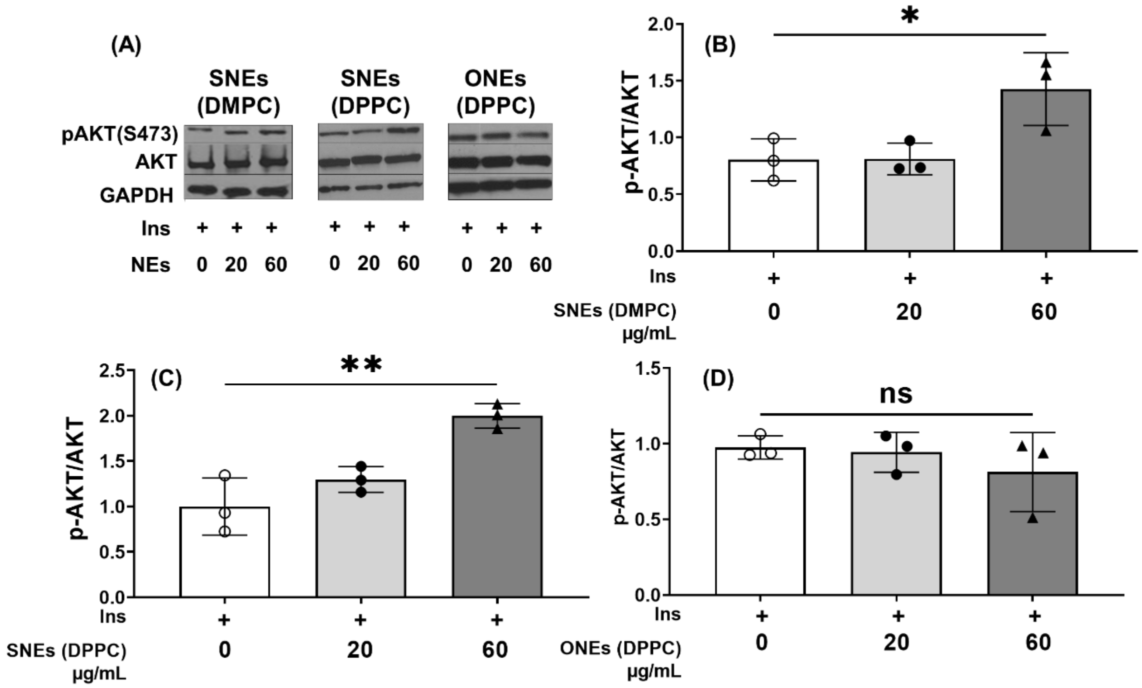

Figure 15. Effect of nanoemulsions on insulin signaling

The hCMEC/D3 cells treated with various concentrations of nanoemulsions (0, 20, 60 µg/mL) followed by insulin stimulation (100 nM, 20 min) were lysed using RIPA buffer and analyzed by western blotting. The GAPDH expression was used as a loading control. The average of p-AKT/total AKT ratios obtained from three independent experiments are presented as the bar chart. (A) Representative blots of pAKT(s473), total AKT and GAPDH. Densitometric analysis of p-AKT/AKT using Image J software shows an increase in pAKT/AKT expression in hCMEC/D3 monolayers after 1 hour incubation with 60 µg/mL SNEs [DOTAP: DMPC (7:1 w/w); B] or SNEs [DOTAP: DPPC (7:1 w/w); C]. No statistically significant differences were found in hCMEC/D3 monolayers with 1-hour pretreatment of ONEs [DOTAP: DPPC (3:1 w/w); D]. Data was normalized to control (insulin alone) and presented as mean ± SD (n = 3); *P<0.05, **p<0.01 one-way ANOVA followed by Bonferroni post-tests.

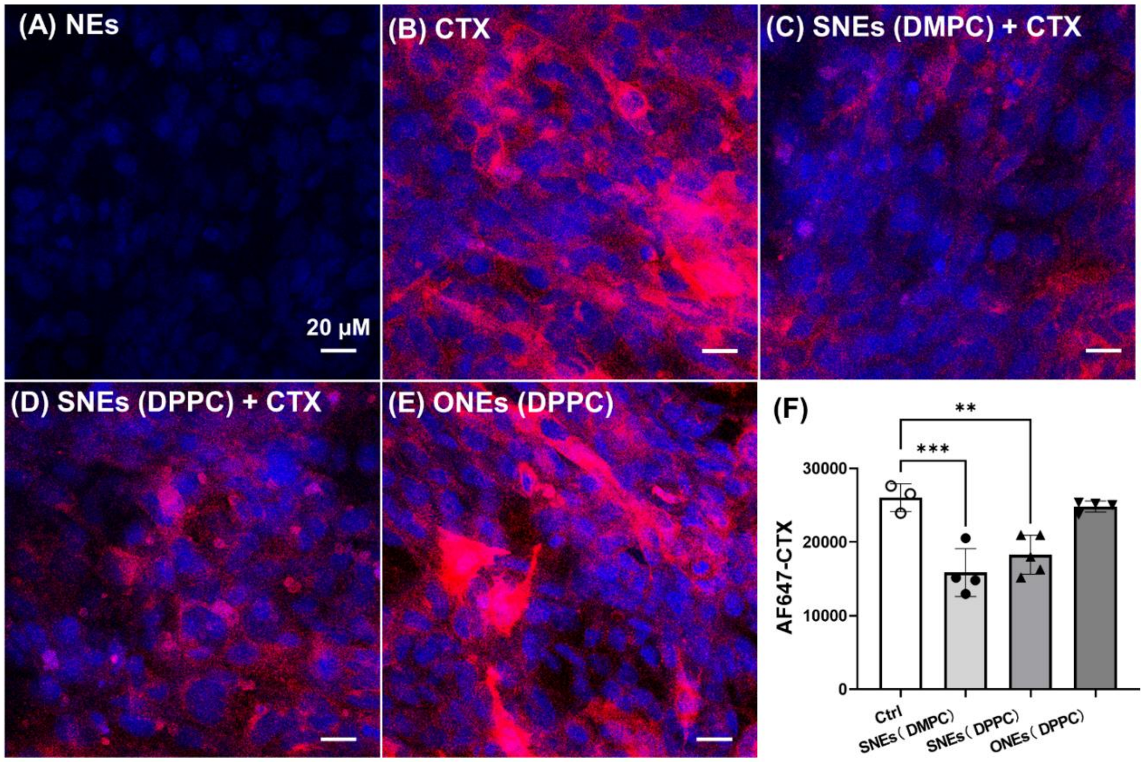

Figure 16. Effect of nanoemulsions on lipid raft integrity in hCMEC/D3 monolayers

Laser confocal micrographs of hCMEC/D3 monolayers treated with nanoemulsions alone (A). B-E: The monolayers were pretreated with 60 µg/mL medium control (B), SNEs [DOTAP: DMPC (7:1 w/w); C], SNEs [DOTAP: DPPC (7:1 w/w); D], or ONEs [DOTAP: DPPC (3:1 w/w; E] followed by 30 min incubation with 5 µg/mL AF647 conjugated Cholera Toxin Subunit B (AF647-CXT) at 37 ^oC. SNEs show reduced AF647-CXT labeling when compared with cells treated with AF647-CXT alone. However, ONEs didn't show any effect on AF647-CXT labeling in hCMEC/D3 monolayer. Red = AF647-CXT; blue = DAPI-stained nuclei. Scale bar, 20 µm. (F) Intracellular fluorescence intensities were quantified using ImageJ software and presented as mean ± S.D. One-way ANOVA followed by Bonferroni post tests showed a significant decrease in AF647-CXT labeling in cells pretreated with SNEs compared to the monolayers pre-treated with the medium However, no change in AF647-CXT labeling was observed in ONE pre-treated cells compared to cells pre-treated with medium alone (**P < 0.01, ***<0.005 one-way ANOVA followed by Bonferroni post-tests).

4. Discussion

Decreased brain insulin levels, insulin receptor deficiency, and insulin signaling disruptions are associated with BBB dysfunction in both metabolic disorders like type 2 diabetes mellitus (T2DM) and neurodegenerative diseases such as AD (Ho, Qin et al. 2004, Lim, Calon et al. 2005, Wang, Ho et al. 2005, Arnold, Arvanitakis et al. 2018). Increased consumption of diet rich in saturated fatty acids was shown to increase the severity of these changes in addition to generating whole body insulin resistance (Koska, Ozias et al. 2016). Substituting saturated FAs (SFAs) with UFAs has been claimed to have beneficial effects on insulin sensitivity (Vessby, Uusitupa et al. 2001, Lovejoy, Smith et al. 2002) and neuropathological changes (Abuznait, Qosa et al. 2013). The UFAs were shown to modulate cell membrane composition, enhance its fluidity, and further regulate signaling events (Bickel 2002, Maulucci, Cohen et al. 2016). Despite these claims, fish oil supplementation, which includes substantial UFAs, failed to affect insulin sensitivity in healthy individuals (Giacco, Cuomo et al. 2007). Interestingly, the level of cerebral DHA did not return to normal after another eight weeks PUFAs feeding, indicating that dietary supply is inefficient and can only cause minor changes in brain lipid composition (Moriguchi, Loewke et al. 2001). Intravenous administration of lipid emulsions is an alternative option to improve the lipid composition of the BBB endothelium and to directly deliver UFAs to the brain. However, these lipid emulsions must be carefully targeted, otherwise they may lead to the elevation of free fatty acid levels in the plasma and cause peripheral endothelial dysfunction (Steinberg, Paradisi et al. 2000, Umpierrez, Smiley et al. 2009, Gosmanov, Smiley et al. 2010, Gosmanov, Smiley et al. 2012).

In this study, we developed nanoemulsions to deliver UFAs to hCMEC/D3 cells and examined their role in regulation of insulin signaling/trafficking and lipid rafts at the BBB. Moreover, the ability of nanoemulsions to transport across the hCMEC/D3 cell monolayers was also investigated. The surfactant ratio was optimized to obtain nanoemulsions with a size range of 150 ~ 200 nm and a positive zeta potential for their optimal cellular uptake without cell toxicity (**Table 5**). Finally, SNEs with DOTAP: DMPC/ DOTAP: DPPC = 7:1 and ONEs with DOTAP: DPPC = 3:1 was considered due to their narrow size distribution with relatively low polydispersity index (PDI) [0.278 ± 0.03 for SNEs (DOTAP: DMPC 7:1 w/w); 0.251 ± 0.03 for SNEs (DOTAP: DPPC 7:1 w/w); and 0.308 ± 0.04 for ONEs (DOTAP: DPPC 3:1 w/w)]. Since DMPC and DPPC have the same head group, which is expected interact similarly with the cell surface receptors, it is unlikely that the small difference in chain length could significantly affect the cellular internalization of nanoparticles, as they all have similar sizes and zeta potential.

Conc. of SNEs (DMPC; μg/mL)	**Live %**
0	95.45
2	96.78
5	95.38
30	98.34
60	94.42

Table 5. Live/dead cell assay of SNEs (DMPC)

The formulated nanoemulsions were stored in the refrigerator (2-6 ^{o}C) and used for experiments within 2 to 3 weeks. Due to their nano size range, the nanoemulsions have relatively higher kinetic stability than conventional emulsions; no significant changes in the particle size range and zeta potential (<± 5 mv) were observed within 2-3 weeks. However, phase separation of the samples was observed beyond a month in storage. Significant broadening of particle size distribution was observed with higher PDI and changes in zeta potential (± 10 mv).

To elucidate the effect of UFAs on insulin signaling and trafficking at the BBB endothelium, SNEs or ONEs containing substantial amounts of a variety of UFAs were employed. The SNEs consist of 62.1% PUFAs (C18:2 ω-6) and ONEs consist of predominantly MUFAs (~67.8%; C18:1 ω-9) (Hwang, Jun et al. 2010). Both SNEs and ONEs were prepared according to established procedures, and their effect on the hCMEC/D3 monolayers was examined. These cells are suitable models for BBB relevant studies, since their transcriptomic (Kalari, Thompson et al. 2016) and proteomic (Ohtsuki, Ikeda et al. 2013) profiles coincide with that of primary human BBB cells. Uptake of both SNEs and ONEs by hCMEC/D3 cells was confirmed by flow cytometry. Incubation of hCMEC/D3 cells with the increasing concentration of both SNEs and ONEs led to an enhanced cellular uptake of nanoemulsions. In line with the cellular uptake determined by flow cytometry, the Z-stack confocal image of the internalized DiI-labeled nanoemulsions revealed tracts of SNE [DOTAP: DMPC (7:1 w/w)], SNEs [DOTAP: DPPC (7:1 w/w)] and ONEs [DOTAP: DPPC (3:1 w/w)] permeation from luminal (plasma) to the abluminal (brain) side of the endothelium. Overall, these results indicate that both SNEs and ONEs are effectively internalized and transported at the BBB endothelium.

SNE pre-treated cells (both DMPC and DPPC formulations) showed higher AF647-insulin uptake compared to the cells treated with the blank medium. In contrast, ONE pre-treatment did not show significant effect on AF647-insulin uptake. This difference may be due to differential effects of PUFA versus MUFA on the morphology of lipid rafts, which mediate caveolae mediated endocytosis of insulin (Lajoie and Nabi 2010, Stralfors 2012, Filippini and D'Alessio 2020). The lipid composition and fluidity of cell membranes is continuously modulated in response to changes in the surrounding environment by adjusting the length and degree of unsaturation of fatty acids (Maulucci, Cohen et al. 2016). The cell membrane exposed to SFAs is less fluid and less responsive to changes in the extracellular environment. The formation of cholesterol-rich domains and disruption of cell membrane structure upon SFA exposure could influence endothelial function and activate inflammatory cells (Cohen, Combs et al. 2003, Mason and Jacob 2003). Substitution of

SFAs by MUFAs improved systemic insulin sensitivity in humans (Vessby, Uusitupa et al. 2001). The cell membrane exposed to unsaturated fatty acids (UFA), such as PUFAs or MUFAs, is more fluid and more responsive (Maulucci, Cohen et al. 2016). Supplementation with ω-3 PUFAs also improved lipoprotein profile and insulin sensitivity in an insulin resistant mouse model (Lucero, Olano et al. 2017). In addition, intracerebroventricular injections of oleic acids (ω-9 MUFAs) in Sprague-Dawley rats enhanced peripheral insulin sensitivity (Obici, Feng et al. 2002). Andreone et al.(Andreone, Chow et al. 2017) demonstrated that docosahexaenoic acid (DHA) enrichment in the cell membrane could inhibit caveolae formation by displacing cholesterol and caveolin-1, thereby increasing membrane fluidity. Moreover, a close association between membrane lipid composition and insulin sensitivity has been observed in both animal models and humans. The elevated membrane viscosity was shown to impair the activation of the hepatic insulin receptor kinase in ageing rats (Nadiv, Shinitzky et al. 1994). These observations indicate that the modifications of membrane lipid composition could profoundly modulate insulin action by altering membrane fluidity, and increase the expression, affinity, and insulin receptor density (Das 2005). Since ONEs, containing MUFAs, did not alter insulin signaling/trafficking, and based on the earlier observation that the cell membrane composition regulation is especially sensitive to ω-6 and ω-3 PUFAs from dietary fat, it is reasonable to assume that PUFAs could outperform MUFAs in altering cell membrane fluidity.

The current study shows that PUFA exposure stimulates insulin signaling by increasing p-AKT/AKT expression. Phosphorylation of AKT in cells pretreated with SNEs [DOTAP: DMPC (7:1 w/w)] was significantly higher compared to the cells pretreated with insulin alone. Similar to SNEs [DOTAP: DMPC (7:1 w/w)], the SNE [DOTAP: DPPC (7:1 w/w)] pretreated cells showed ~2-fold increase in AKT phosphorylation compared to control cells. However, no changes in AKT phosphorylation were observed in the cells pre-treated with ONEs [DOTAP: DPPC (3:1 w/w)] compared to the control cells. This indicates a further association between PUFAs and BBB insulin signaling. The lack of observable impact of MUFAs on insulin signaling may be attributed to their modest effect on the lipid rafts. Using laser confocal microscopy, we have shown that the labeling of lipid rafts by AF647-CXT in polarized hCMEC/D3 cell monolayers was disrupted by SNEs but not by ONEs. Cholera toxin subunit B can bind to ganglioside GM1 and is widely used as a marker for lipid rafts. Our results showed that SNEs alter lipid raft morphology, most likely by modulating sphingolipids (Kabbani, Raghunathan et al. 2020) and cholesterol in the lipid rafts (Basiouni, Stockel et al. 2012, Shaikh 2012, Turk and Chapkin 2013) and regulating the signaling of receptors located in the lipid rafts. SNEs containing PUFAs may provide positive benefits in various disease conditions by reducing the number or volume of lipid rafts present in the brain endothelial cell membranes.

5. Conclusion and future work

The current study indicates that increase membrane fluidity and enhance insulin signaling and trafficking at the BBB. By so doing the SNEs could rekindle insulin signaling at the BBB, reach the brain, and manifest similar effects in the brain parenchyma. The delivery of nanoemulsions containing PUFAs might represent a non-pharmacological approach to ameliorate various metabolic, vascular, and neurodegenerative pathologies by improving membrane lipid composition and rectifying the aberrant trafficking/signaling of insulin (**Figure 14**).

In the future, further studies are needed to investigate how these formulated nanoemulsions are transported into the BBB and by which mechanism they can regulate insulin signaling and trafficking at the BBB. Moreover, some other groups also emphasized the importance of ω-3/ ω-6 PUFA ratio on BBB function. Therefore, the oil core of the nanoemulsions needs to be optimized.

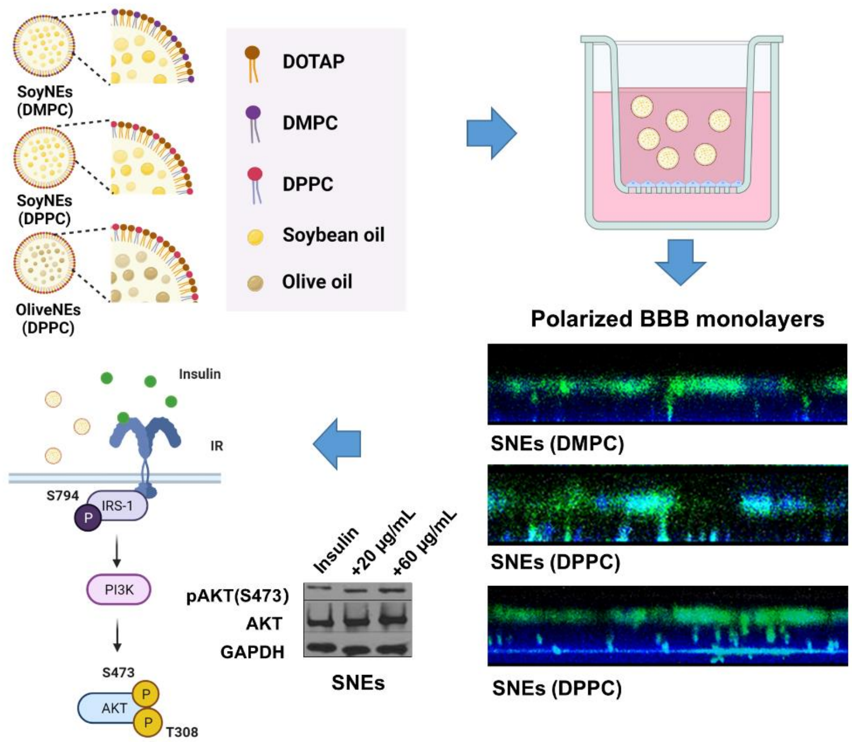

Figure 17. Summary plot showing SNEs containing UFAs are taken up by the polarized BBB endothelial monolayers, where they increase insulin signaling and trafficking.

6. Abbreviation

Central nervous system	CNS
Blood-brain barrier	BBB
Type II diabetes	T2D
Alzheimer’s disease	AD
Phosphatidylcholine	PC
Phosphatidylethanolamine	PE

Phosphatidylethanolamine plasmalogen	PEpl
Phosphatidylserine	PS
Phosphatidylinositol	PI
Cardiolipin	CL
Fatty acids	FAs
Saturated FAs	SFAs
Monounsaturated FAs	MUFAs
Polyunsaturated FAs	PUFAs
Palmitic acid	PAA (C16:0)
Stearic acid	SA (C18:0)
Oleic acids	OA (C18:1)
α-linolenic acid	ALA (C18:3)
Eicosapentaenoic acid	EPA (C20:5)
Docosahexaenoic acid	DHA (C22:6)
Linoleic acid	LA (C18:2)
Arachidonic acid	AA (C20:4)
Docosapentaenoic acid	DPA (C22:5)
Lysophospholipid	LPL
Fatty acid transportation proteins	FATPs
Fatty acid translocase	FAT/CD36

Major facilitator superfamily domain-containing protein	Mfsd2a
Low-density lipoprotein	LDL
High-density lipoproteins like apolipoprotein A-1	ApoA-1
1,1'dioctadecyl-3,3,3',3'-tetramethyl indocarbocyanine	DiI-C18
1, 2-dimyristoyl-sn-glycero-3-phosphatidylcholine	DMPC
1,2-dipalmitoyl-sn-glycero-3-phosphocholine	DPPC
1,2-dioleoyl-3-trimethylammonium-propane as a chloride salt	DOTAP
Basic fibroblast growth factor	bFGF
Fetal bovine serum	FBS
Dulbecco's phosphate buffered saline	DPBS
Human cerebral microvascular endothelial cell line	hCMEC/D3
Alexa Fluor 647-labeled insulin	AF647-insulin
radio-immunoprecipitation assay	RIPA
Bicinchoninic acid assay	BCA assay
AF647 conjugated Cholera Toxin Subunit B	AF647-CXT

7. Bibliography

Aboudzadeh, M. A. and S. Hamzehlou (2020). Low-Energy Emulsification Methods for Encapsulation of Antioxidants, Springer, Cham.

Abuznait, A. H., H. Qosa, B. A. Busnena, K. A. El Sayed and A. Kaddoumi (2013). "Olive-oil-derived oleocanthal enhances beta-amyloid clearance as a potential neuroprotective mechanism against Alzheimer's disease: in vitro and in vivo studies." ACS Chem Neurosci **4**(6): 973-982.

Aksoylu Özbek, Z., P. Günç Ergönül and M. A. Aboudzadeh (2020). High-Energy Emulsification Methods for Encapsulation of Lipid-Soluble Antioxidants. Food Bioactive Ingredients, Springer, Cham.

Andreone, B. J., B. W. Chow, A. Tata, B. Lacoste, A. Ben-Zvi, K. Bullock, A. A. Deik, D. D. Ginty, C. B. Clish and C. Gu (2017). "Blood-Brain Barrier Permeability Is Regulated by Lipid Transport-Dependent Suppression of Caveolae-Mediated Transcytosis." Neuron **94**(3): 581-594 e585.

Andreone, B. J., B. Lacoste and C. Gu (2015). "Neuronal and vascular interactions." Annu Rev Neurosci **38**(1545-4126): 25-46.

Arnold, S. E., Z. Arvanitakis, S. L. Macauley-Rambach, A. M. Koenig, H. Y. Wang, R. S. Ahima, S. Craft, S. Gandy, C. Buettner, L. E. Stoeckel, D. M. Holtzman and D. M. Nathan (2018). "Brain insulin resistance in type 2 diabetes and Alzheimer disease: concepts and conundrums." Nat Rev Neurol **14**(3): 168-181.

Basiouni, S., K. Stockel, H. Fuhrmann and J. Schumann (2012). "Polyunsaturated fatty acid supplements modulate mast cell membrane microdomain composition." Cell Immunol **275**(1-2): 42-46.

Benistant, C., M. P. Dehouck, J. C. Fruchart, R. Cecchelli and M. Lagarde (1995). "Fatty acid composition of brain capillary endothelial cells: effect of the coculture with astrocytes." J Lipid Res **36**(11): 2311-2319.

Bezard, J., J. P. Blond, A. Bernard and P. Clouet (1994). "The metabolism and availability of essential fatty acids in animal and human tissues." Reprod Nutr Dev **34**(6): 539-568.

Bhattacharjee, S. (2016). "DLS and zeta potential - What they are and what they are not?" J Control Release **235**: 337-351.

Bickel, P. E. (2002). "Lipid rafts and insulin signaling." Am J Physiol Endocrinol Metab **282**(1): E1-E10.

Bourre, J. M., G. Durand, G. Pascal and A. Youyou (1989). "Brain cell and tissue recovery in rats made deficient in n-3 fatty acids by alteration of dietary fat." J Nutr **119**(1): 15-22.

Bourre, J. M. and M. Piciotti (1992). "Delta-6 desaturation of alpha-linolenic acid in brain and liver during development and aging in the mouse." Neurosci Lett **141**(1): 65-68.

Brinkmann, J. F., N. A. Abumrad, A. Ibrahimi, G. J. van der Vusse and J. F. Glatz (2002). "New insights into long-chain fatty acid uptake by heart muscle: a crucial role for fatty acid translocase/CD36." Biochem J **367**(Pt 3): 561-570.

Campbell, S. D., K. J. Regina and E. D. Kharasch (2014). "Significance of lipid composition in a blood-brain barrier-mimetic PAMPA assay." J Biomol Screen **19**(3): 437-444.

Cermenati, G., N. Mitro, M. Audano, R. C. Melcangi, M. Crestani, E. De Fabiani and D. Caruso (2015). "Lipids in the nervous system: from biochemistry and molecular biology to patho-physiology." Biochim Biophys Acta **1851**(1): 51-60.

Chew, H., V. A. Solomon and A. N. Fonteh (2020). "Involvement of Lipids in Alzheimer's Disease Pathology and Potential Therapies." Front Physiol **11**(1664-042X): 598.

Cisa-Wieczorek, S. and M. I. Hernandez-Alvarez (2020). "Deregulation of Lipid Homeostasis: A Fa(c)t in the Development of Metabolic Diseases." Cells **9**(12): 2605.

Cohen, A. W., T. P. Combs, P. E. Scherer and M. P. Lisanti (2003). "Role of caveolin and caveolae in insulin signaling and diabetes." Am J Physiol Endocrinol Metab **285**(6): E1151-1160.

Connor, W. E., M. Neuringer and D. S. Lin (1990). "Dietary effects on brain fatty acid composition: the reversibility of n-3 fatty acid deficiency and turnover of docosahexaenoic acid in the brain, erythrocytes, and plasma of rhesus monkeys." J Lipid Res **31**(2): 237-247.

Dai, Y. J., L. L. Sun, M. Y. Li, C. L. Ding, Y. C. Su, L. J. Sun, S. H. Xue, F. Yan, C. H. Zhao and W. Wang (2016). "Comparison of Formulas Based on Lipid Emulsions of Olive Oil, Soybean Oil, or Several Oils for Parenteral Nutrition: A Systematic Review and Meta-Analysis." Adv Nutr **7**(2): 279-286.

Daneman, R. and A. Prat (2015). "The blood-brain barrier." Cold Spring Harb Perspect Biol **7**(1): a020412.

Das, U. N. (2005). "A defect in the activity of Delta6 and Delta5 desaturases may be a factor predisposing to the development of insulin resistance syndrome." Prostaglandins Leukot Essent Fatty Acids **72**(5): 343-350.

Day, C. A. and A. K. Kenworthy (2015). "Functions of cholera toxin B-subunit as a raft cross-linker." Essays Biochem **57**: 135-145.

Delion, S., S. Chalon, D. Guilloteau, B. Lejeune, J. C. Besnard and G. Durand (1997). "Age-related changes in phospholipid fatty acid composition and monoaminergic neurotransmission in the hippocampus of rats fed a balanced or an n-3 polyunsaturated fatty acid-deficient diet." J Lipid Res **38**(4): 680-689.

Diaz, M., N. Fabelo, V. Casanas-Sanchez, R. Marin, T. Gomez, D. Quinto-Alemany and J. A. Perez (2016). "Hippocampal Lipid Homeostasis in APP/PS1 Mice is Modulated by a Complex Interplay Between Dietary DHA and Estrogens: Relevance for Alzheimer's Disease." J Alzheimers Dis **49**(2): 459-481.

Dinh, L., J. M. Bourre, O. Dumont and G. Durand (1995). "Comparison of recovery of previously depressed hepatic delta 6 desaturase activity in adult and old rats." Ann Nutr Metab **39**(2): 117-123.

Edmond, J. (2001). "Essential polyunsaturated fatty acids and the barrier to the brain: the components of a model for transport." J Mol Neurosci **16**(2-3): 181-193; discussion 215-121.

Fahy, E., S. Subramaniam, R. C. Murphy, M. Nishijima, C. R. Raetz, T. Shimizu, F. Spener, G. van Meer, M. J. Wakelam and E. A. Dennis (2009). "Update of the LIPID MAPS comprehensive classification system for lipids." J Lipid Res **50 Suppl**(0022-2275): S9-14.

Farooqui, A. A., L. Liss and L. A. Horrocks (1988). "Neurochemical aspects of Alzheimer's disease: involvement of membrane phospholipids." Metab Brain Dis **3**(1): 19-35.

Filippini, A. and A. D'Alessio (2020). "Caveolae and Lipid Rafts in Endothelium: Valuable Organelles for Multiple Functions." Biomolecules **10**(9): 1218.

Filippini, A. A.-O. X. and A. A.-O. D'Alessio "Caveolae and Lipid Rafts in Endothelium: Valuable Organelles for Multiple Functions. LID - 10.3390/biom10091218 [doi] LID - 1218." (2218-273X (Electronic)).

Flanagan, J., K. Kortegaard, D. Neil Pinder, T. Rades and H. Singh (2006). "Solubilisation of soybean oil in microemulsions using various surfactants." Food Hydrocolloids **20**(2-3): 253-260.

Ganta, S., D. Deshpande, A. Korde and M. Amiji (2010). "A review of multifunctional nanoemulsion systems to overcome oral and CNS drug delivery barriers." Mol Membr Biol **27**(7): 260-273.

Gao, F., A. Y. Taha, K. Ma, L. Chang, D. Kiesewetter and S. I. Rapoport (2013). "Aging decreases rate of docosahexaenoic acid synthesis-secretion from circulating unesterified alpha-linolenic acid by rat liver." Age (Dordr) **35**(3): 597-608.

Giacco, R., V. Cuomo, B. Vessby, M. Uusitupa, K. Hermansen, B. J. Meyer, G. Riccardi and A. A. Rivellese (2007). "Fish oil, insulin sensitivity, insulin secretion and glucose tolerance in healthy people: is there any effect of fish oil supplementation in relation to the type of background diet and habitual dietary intake of n-6 and n-3 fatty acids?" Nutr Metab Cardiovasc Dis **17**(8): 572-580.

Gosmanov, A. R., D. D. Smiley, L. Peng, J. Siquiera, G. Robalino, C. Newton and G. E. Umpierrez (2012). "Vascular effects of intravenous intralipid and dextrose infusions in obese subjects." Metabolism **61**(10): 1370-1376.

Gosmanov, A. R., D. D. Smiley, G. Robalino, J. Siquiera, B. Khan, N. A. Le, R. S. Patel, A. A. Quyyumi, L. Peng, A. E. Kitabchi and G. E. Umpierrez (2010). "Effects of oral and intravenous fat load on blood pressure, endothelial function, sympathetic activity, and oxidative stress in obese healthy subjects." Am J Physiol Endocrinol Metab **299**(6): E953-958.

Gramlich, L., C. Ireton-Jones, J. M. Miles, M. Morrison and A. Pontes-Arruda (2019). "Essential Fatty Acid Requirements and Intravenous Lipid Emulsions." JPEN J Parenter Enteral Nutr **43**(6): 697-707.

Hachem, M., M. Belkouch, A. Lo Van, M. Picq, N. Bernoud-Hubac and M. Lagarde (2020). "Brain targeting with docosahexaenoic acid as a prospective therapy for neurodegenerative diseases and its passage across blood brain barrier." Biochimie **170**: 203-211.

Hadders-Algra, M. (2008). "Prenatal long-chain polyunsaturated fatty acid status: the importance of a balanced intake of docosahexaenoic acid and arachidonic acid." J Perinat Med **36**(2): 101-109.

Hamilton, J. A. and K. Brunaldi (2007). "A model for fatty acid transport into the brain." J Mol Neurosci **33**(1): 12-17.

Hancock, S. E., M. G. Friedrich, T. W. Mitchell, R. J. Truscott and P. L. Else (2015). "Decreases in Phospholipids Containing Adrenic and Arachidonic Acids Occur in the Human Hippocampus over the Adult Lifespan." Lipids **50**(9): 861-872.

Hancock, S. E., M. G. Friedrich, T. W. Mitchell, R. J. Truscott and P. L. Else (2017). "The phospholipid composition of the human entorhinal cortex remains relatively stable over 80 years of adult aging." Geroscience **39**(1): 73-82.

Ho, L., W. Qin, P. N. Pompl, Z. Xiang, J. Wang, Z. Zhao, Y. Peng, G. Cambareri, A. Rocher, C. V. Mobbs, P. R. Hof and G. M. Pasinetti (2004). "Diet-induced insulin resistance promotes amyloidosis in a transgenic mouse model of Alzheimer's disease." FASEB J **18**(7): 902-904.

Hooijmans, C. R. and A. J. Kiliaan (2008). "Fatty acids, lipid metabolism and Alzheimer pathology." Eur J Pharmacol **585**(1): 176-196.

Hwang, J., H. S. Jun and E. Shim (2010). "Rates of Change in Tissue Fatty Acid Composition When Dietary Soybean Oil Is Switched to Olive Oil." Journal of Health Science **56**(3): 275-286.

Kabbani, A. M., K. Raghunathan, W. I. Lencer, A. K. Kenworthy and C. V. Kelly (2020). "Structured clustering of the glycosphingolipid GM1 is required for membrane curvature induced by cholera toxin." Proceedings of the National Academy of Sciences of the United States of America **117**(26): 14978-14986.

Kalari, K. R., K. J. Thompson, A. A. Nair, X. Tang, M. A. Bockol, N. Jhawar, S. K. Swaminathan, V. J. Lowe and K. K. Kandimalla (2016). "BBBomics-Human Blood Brain Barrier Transcriptomics Hub." Front Neurosci **10**: 71.

Karmi, A., P. Iozzo, A. Viljanen, J. Hirvonen, B. A. Fielding, K. Virtanen, V. Oikonen, J. Kemppainen, T. Viljanen, L. Guiducci, M. Haaparanta-Solin, K. Nagren, O. Solin and P. Nuutila (2010). "Increased brain fatty acid uptake in metabolic syndrome." Diabetes **59**(9): 2171-2177.

Koska, J., M. K. Ozias, J. Deer, J. Kurtz, A. D. Salbe, S. M. Harman and P. D. Reaven (2016). "A human model of dietary saturated fatty acid induced insulin resistance." Metabolism **65**(11): 1621-1628.

Koundouros, N. and G. Poulogiannis (2020). "Reprogramming of fatty acid metabolism in cancer." Br J Cancer **122**(1): 4-22.

Kumar, M., R. S. Bishnoi, A. K. Shukla and C. P. Jain (2019). "Techniques for Formulation of Nanoemulsion Drug Delivery System: A Review." Prev Nutr Food Sci **24**(3): 225-234.

Lajoie, P. and I. R. Nabi (2010). Lipid Rafts, Caveolae, and Their Endocytosis. International Review of Cell and Molecular Biology. K. W. Jeon, Academic Press. **282:** 135-163.

Lim, G. P., F. Calon, T. Morihara, F. Yang, B. Teter, O. Ubeda, N. Salem, Jr., S. A. Frautschy and G. M. Cole (2005). "A diet enriched with the omega-3 fatty acid docosahexaenoic acid reduces amyloid burden in an aged Alzheimer mouse model." J Neurosci **25**(12): 3032-3040.

Little, S. J., M. A. Lynch, M. Manku and A. Nicolaou (2007). "Docosahexaenoic acid-induced changes in phospholipids in cortex of young and aged rats: a lipidomic analysis." Prostaglandins Leukot Essent Fatty Acids **77**(3-4): 155-162.

Lovejoy, J. C., S. R. Smith, C. M. Champagne, M. M. Most, M. Lefevre, J. P. DeLany, Y. M. Denkins, J. C. Rood, J. Veldhuis and G. A. Bray (2002). "Effects of diets enriched in saturated (palmitic), monounsaturated (oleic), or trans (elaidic) fatty acids on insulin sensitivity and substrate oxidation in healthy adults." Diabetes Care **25**(8): 1283-1288.

Lucero, D., C. Olano, M. Bursztyn, C. Morales, A. Stranges, S. Friedman, E. V. Macri, L. Schreier and V. Zago (2017). "Supplementation with n-3, n-6, n-9 fatty acids in an insulin-resistance animal model: does it improve VLDL quality?" Food Funct **8**(5): 2053-2061.

Martin, V., N. Fabelo, G. Santpere, B. Puig, R. Marin, I. Ferrer and M. Diaz (2010). "Lipid alterations in lipid rafts from Alzheimer's disease human brain cortex." J Alzheimers Dis **19**(2): 489-502.

Mason, R. P. and R. F. Jacob (2003). "Membrane microdomains and vascular biology: emerging role in atherogenesis." Circulation **107**(17): 2270-2273.

Maulucci, G., O. Cohen, B. Daniel, A. Sansone, P. I. Petropoulou, S. Filou, A. Spyridonidis, G. Pani, M. De Spirito, C. Chatgilialoglu, C. Ferreri, K. E. Kypreos and S. Sasson (2016). "Fatty acid-related modulations of membrane fluidity in cells: detection and implications." Free Radic Res **50**(sup1): S40-S50.

McNamara, R. K., Y. Liu, R. Jandacek, T. Rider and P. Tso (2008). "The aging human orbitofrontal cortex: decreasing polyunsaturated fatty acid composition and associated increases in lipogenic gene expression and stearoyl-CoA desaturase activity." Prostaglandins Leukot Essent Fatty Acids **78**(4-5): 293-304.

Melanie, L. (2020). "Snapshot Analysis: Nano-emulsification Formulation Technology." from https://ascensionsciences.com/newsroom/technical-articles/snapshot-analysis-nano-emulsification-formulation-technology/.

Mesa-Herrera, F., L. Taoro-Gonzalez, C. Valdes-Baizabal, M. Diaz and R. Marin (2019). "Lipid and Lipid Raft Alteration in Aging and Neurodegenerative Diseases: A Window for the Development of New Biomarkers." Int J Mol Sci **20**(15): 3810.

Mitchell, R. W., N. H. On, M. R. Del Bigio, D. W. Miller and G. M. Hatch (2011). "Fatty acid transport protein expression in human brain and potential role in fatty acid transport across human brain microvessel endothelial cells." J Neurochem **117**(4): 735-746.

Moore, S. A. (1993). "Cerebral endothelium and astrocytes cooperate in supplying docosahexaenoic acid to neurons." Adv Exp Med Biol **331**(0065-2598 (Print)): 229-233.

Moore, S. A., E. Yoder, S. Murphy, G. R. Dutton and A. A. Spector (1991). "Astrocytes, not neurons, produce docosahexaenoic acid (22:6 omega-3) and arachidonic acid (20:4 omega-6)." J Neurochem **56**(2): 518-524.

Moore, S. A., E. Yoder and A. A. Spector (1990). "Role of the blood-brain barrier in the formation of long-chain omega-3 and omega-6 fatty acids from essential fatty acid precursors." J Neurochem **55**(2): 391-402.

Moriguchi, T., J. Loewke, M. Garrison, J. N. Catalan and N. Salem, Jr. (2001). "Reversal of docosahexaenoic acid deficiency in the rat brain, retina, liver, and serum." J Lipid Res **42**(3): 419-427.

Nadiv, O., M. Shinitzky, H. Manu, D. Hecht, C. T. Roberts, Jr., D. LeRoith and Y. Zick (1994). "Elevated protein tyrosine phosphatase activity and increased membrane viscosity are associated with impaired activation of the insulin receptor kinase in old rats." Biochem J **298 (Pt 2)**(2): 443-450.

Naudi, A., R. Cabre, M. Jove, V. Ayala, H. Gonzalo, M. Portero-Otin, I. Ferrer and R. Pamplona (2015). "Lipidomics of human brain aging and Alzheimer's disease pathology." Int Rev Neurobiol **122**(2162-5514): 133-189.

Nikolić, I., A. Gledović, S. Tamburić, T. Major and S. S. (2020). Nanoemulsions as Carriers for Natural Antioxidants: Formulation Development and Optimisation. Food Bioactive Ingredients, Springer, Cham.

Norris, S. E., M. G. Friedrich, T. W. Mitchell, R. J. W. Truscott and P. L. Else (2015). "Human prefrontal cortex phospholipids containing docosahexaenoic acid increase during normal adult aging, whereas those containing arachidonic acid decrease." Neurobiol Aging **36**(4): 1659-1669.

Obici, S., Z. Feng, K. Morgan, D. Stein, G. Karkanias and L. Rossetti (2002). "Central administration of oleic acid inhibits glucose production and food intake." Diabetes **51**(2): 271-275.

Ohtsuki, S., C. Ikeda, Y. Uchida, Y. Sakamoto, F. Miller, F. Glacial, X. Decleves, J. M. Scherrmann, P. O. Couraud, Y. Kubo, M. Tachikawa and T. Terasaki (2013). "Quantitative targeted absolute proteomic analysis of transporters, receptors and junction proteins for validation of human cerebral microvascular endothelial cell line hCMEC/D3 as a human blood-brain barrier model." Mol Pharm **10**(1): 289-296.

Pan, Y., H. Khalil and J. A. Nicolazzo (2015). "The Impact of Docosahexaenoic Acid on Alzheimer's Disease: Is There a Role of the Blood-Brain Barrier?" Curr Clin Pharmacol **10**(3): 222-241.

Perona, J. S. (2017). "Membrane lipid alterations in the metabolic syndrome and the role of dietary oils." Biochim Biophys Acta Biomembr **1859**(9 Pt B): 1690-1703.

Pifferi, F., B. Laurent and M. Plourde (2021). "Lipid Transport and Metabolism at the Blood-Brain Interface: Implications in Health and Disease." Frontiers in Physiology **12**: 407.

Pike, L. J. (2003). "Lipid rafts: bringing order to chaos." J Lipid Res **44**(4): 655-667.

Pike, L. J., X. F. Han, K. F. Chung and R. W. Gross (2002). "Lipid rafts are enriched in arachidonic acid and plasmenylethanolamine and their composition is independent of caveolin-1 expression: a quantitative electrospray ionization/mass spectrometric analysis." Biochemistry **41**(6): 2075-2088.

Pu, L., U. Igbavboa, W. G. Wood, J. B. Roths, A. B. Kier, F. Spener and F. Schroeder (1999). "Expression of fatty acid binding proteins is altered in aged mouse brain." Mol Cell Biochem **198**(1-2): 69-78.

Qian, C. and D. J. McClements (2011). "Formation of nanoemulsions stabilized by model food-grade emulsifiers using high-pressure homogenization: Factors affecting particle size." Food Hydrocolloids **25**(5): 1000-1008.

Rouser, G. and A. Yamamoto (1968). "Curvilinear regression course of human brain lipid composition changes with age." Lipids **3**(3): 284-287.

Salvia-Trujillo, L., R. Soliva-Fortuny, M. A. Rojas-Grau, D. J. McClements and O. Martin-Belloso (2017). "Edible Nanoemulsions as Carriers of Active Ingredients: A Review." Annu Rev Food Sci Technol **8**(1941-1413): 439-466.

Shaikh, S. R. (2012). "Biophysical and biochemical mechanisms by which dietary N-3 polyunsaturated fatty acids from fish oil disrupt membrane lipid rafts." J Nutr Biochem **23**(2): 101-105.

Siakotos, A. N. and G. Rouser (1969). "Isolation of highly purified human and bovine brain endothelial cells and nuclei and their phospholipid composition." Lipids **4**(3): 234-239.

Solè, I. and C. Solans (2013). Nanoemulsions. Encyclopedia of Colloid and Interface Science. T. Tadros. Berlin, Heidelberg, Springer Berlin Heidelberg**:** 733-747.

Steinberg, H. O., G. Paradisi, G. Hook, K. Crowder, J. Cronin and A. D. Baron (2000). "Free fatty acid elevation impairs insulin-mediated vasodilation and nitric oxide production." Diabetes **49**(7): 1231-1238.

Stralfors, P. (2012). "Caveolins and caveolae, roles in insulin signalling and diabetes." Adv Exp Med Biol **729**(0065-2598 (Print)): 111-126.

Svennerholm, L., K. Bostrom and B. Jungbjer (1997). "Changes in weight and compositions of major membrane components of human brain during the span of adult human life of Swedes." Acta Neuropathol **94**(4): 345-352.

Swaminathan, S. K., K. M. Ahlschwede, V. Sarma, G. L. Curran, R. S. Omtri, T. Decklever, V. J. Lowe, J. F. Poduslo and K. K. Kandimalla (2018). "Insulin differentially affects the distribution kinetics of amyloid beta 40 and 42 in plasma and brain." J Cereb Blood Flow Metab **38**(5): 904-918.

Takamura, H., H. Kasai, H. Arita and M. Kito (1990). "Phospholipid molecular species in human umbilical artery and vein endothelial cells." J Lipid Res **31**(4): 709-717.

Turk, H. F. and R. S. Chapkin (2013). "Membrane lipid raft organization is uniquely modified by n-3 polyunsaturated fatty acids." Prostaglandins Leukot Essent Fatty Acids **88**(1): 43-47.

Umpierrez, G. E., D. Smiley, G. Robalino, L. Peng, A. E. Kitabchi, B. Khan, A. Le, A. Quyyumi, V. Brown and L. S. Phillips (2009). "Intravenous intralipid-induced blood pressure elevation and endothelial dysfunction in obese African-Americans with type 2 diabetes." J Clin Endocrinol Metab **94**(2): 609-614.

Vainio, S., S. Heino, J. E. Mansson, P. Fredman, E. Kuismanen, O. Vaarala and E. Ikonen (2002). "Dynamic association of human insulin receptor with lipid rafts in cells lacking caveolae." EMBO Rep **3**(1): 95-100.

Vessby, B., M. Uusitupa, K. Hermansen, G. Riccardi, A. A. Rivellese, L. C. Tapsell, C. Nalsen, L. Berglund, A. Louheranta, B. M. Rasmussen, G. D. Calvert, A. Maffetone, E. Pedersen, I. B. Gustafsson and L. H. Storlien (2001). "Substituting dietary saturated for monounsaturated fat impairs insulin sensitivity in healthy men and women: The KANWU Study." Diabetologia **44**(3): 312-319.

Voigt, J., J. Christensen and V. P. Shastri (2014). "Differential uptake of nanoparticles by endothelial cells through polyelectrolytes with affinity for caveolae." Proc Natl Acad Sci U S A **111**(8): 2942-2947.

von Corswant, C. and O. Söderman (1998). "Effect of Adding Isopropyl Myristate to Microemulsions Based on Soybean Phosphatidylcholine and Triglycerides." Langmuir **14**(13): 3506-3511.

Vyas, T. K., A. Shahiwala and M. M. Amiji (2008). "Improved oral bioavailability and brain transport of Saquinavir upon administration in novel nanoemulsion formulations." Int J Pharm **347**(1-2): 93-101.

Wang, J., L. Ho, W. Qin, A. B. Rocher, I. Seror, N. Humala, K. Maniar, G. Dolios, R. Wang, P. R. Hof and G. M. Pasinetti (2005). "Caloric restriction attenuates beta-amyloid neuropathology in a mouse model of Alzheimer's disease." FASEB J **19**(6): 659-661.

Yamanaka, W. K., G. W. Clemans and M. L. Hutchinson (1980). "Essential fatty acids deficiency in humans." Prog Lipid Res **19**(3-4): 187-215.

Zhang, W., R. Chen, T. Yang, N. Xu, J. Chen, Y. Gao and R. A. Stetler (2018). "Fatty acid transporting proteins: Roles in brain development, aging, and stroke." Prostaglandins Leukot Essent Fatty Acids **136**(1532-2823): 35-45.

Zhang, W., R. Chen, T. Yang, N. Xu, J. Chen, Y. Gao and R. A. Stetler (2018). "Fatty acid transporting proteins: Roles in brain development, aging, and stroke." Prostaglandins Leukot Essent Fatty Acids **136**: 35-45.